

Yield Asymmetry Behaviour in Mg-Zr, Mg-Sn and Mg-Zr-Sn alloys

M.Tech. Thesis

By

M SUDHARSANA RAJ



**DEPARTMENT OF METALLURGICAL ENGINEERING
AND MATERIAL SCIENCE
INDIAN INSTITUTE OF TECHNOLOGY
INDORE**

MAY, 2024

Yield Asymmetry Behaviour in Mg-Zr, Mg-Sn and Mg-Zr-Sn alloys

A THESIS

*Submitted in partial fulfillment of the
requirements for the award of the degree
of*
Master of Technology

Submitted by
M SUDHARSANA RAJ
(2202105020)

Under the guidance of
Dr. Dudekula Althaf Basha



**DEPARTMENT OF METALLURGICAL ENGINEERING
AND MATERIAL SCIENCE
INDIAN INSTITUTE OF TECHNOLOGY
INDORE**

MAY, 2024



INDIAN INSTITUTE OF TECHNOLOGY INDORE

CANDIDATE'S DECLARATION

I hereby certify that the work which is being presented in the thesis entitled **Yield Asymmetry Behaviour in Mg-Zr, Mg-Sn and Mg-Zr-Sn alloys** in the partial fulfilment of the requirements for the award of the degree of **MASTER OF TECHNOLOGY** and submitted in the **DEPARTMENT OF METALLURGICAL ENGINEERING AND MATERIAL SCIENCE, Indian Institute of Technology Indore**, is an authentic record of my own work carried out during the time period from August 2022 to June 2024 under the supervision of Dr. Dudekula Althaf Basha, Assistant Professor, Indian Institute of Technology, Indore.

The matter presented in this thesis has not been submitted by me for the award of any other degree of this or any other institute.

M SUDHARSANA RAJ

This is to certify that the above statement made by the candidate is correct to the best of my/our knowledge.

Dr. Dudekula Althaf Basha

M SUDHARSANA RAJ has successfully given his M.Tech. Oral Examination held on **28/05/2024**.

Dr. Dudekula Althaf Basha

Asst. Professor, IIT Indore

Date: 30/05/2024

Convener, DPGC

Dept. of MEMS

Date: 30/05/2024

Acknowledgement

Firstly, I would like to thank my guide, Dr.Dudekula Althaf Basha, for considering me worthy enough to work under him on this project. I thank him for giving me the opportunity and all the necessary support to study the yield asymmetry behavior in Mg-Zr, Mg-Sn and Mg-Zr-Sn alloys.

I am also extremely grateful to the DPGC, Dr Dhirendra Kumar Rai for allowing me to utilize the various academic resources and department facilities at our disposal.

I would also like to thank my friends, Ramamoorthy, Abhinav, Musaib and Aman, who supported me in the toughest of times.

And lastly, I would like to thank those hundreds of scholars who have previously researched and contributed to this field, on whose works this report is based.

With sincerest regards,



M SUDHARSANA RAJ

DEDICATION

This thesis is dedicated to my parents, teachers and friends, whose unwavering support and encouragement have been the bedrock of my educational journey. Their belief in me has been a constant source of motivation. Thank you for your love, patience, and guidance.

ABSTRACT

This project is focused on the study of Mg-Zr, Mg-Sn and Mg-Zr-Sn alloys with the objective of overcoming the limitations of Magnesium due to its crystal structure (HCP). It was carried out through alloying of magnesium in three combinations i.e., Mg-0.3%wtZr, Mg-0.3%wtSn and Mg-0.3%wtZr-0.3%wtSn. The three alloys were prepared using vacuum stir casting at a temperature of 723 K for 4 hours followed by quenching. It was then hot rolled at a temperature of 573 K and at the strain rate of 10^{-3} s^{-1} . The yield asymmetry behaviour of these three alloys was studied.

Through SEM-EBSD analysis the texture and microstructure of three alloys Mg-0.3%wtZr, Mg-0.3%wtSn and Mg-0.3%wtZr-0.3%wtSn were analysed. Through STEM-HAADF imaging and the STEM-EDS line profile analysis the grain boundary segregation of Sn element was observed in ternary alloy Mg-0.3%wtZr-0.3%wtSn and consequently this alloy exhibited low yield asymmetry behaviour.

TABLE OF CONTENTS

PAGE NO

ABSTRACT.....	(iv)
Chapter 1: INTRODUCTION	
1.1.APPLICATIONS OF MAGNESIUM ALLOYS.....	1
1.1.1.AUTOMOTIVE INDUSTRY.....	1
1.1.2.AEROSPACE INDUSTRY.....	1
1.1.3.MEDICAL SECTOR.....	1
1.1.4.ELECTRONICS INDUSTRY.....	1
1.2. LIMITATIONS OF MAGNESIUM ALLOYS.....	2
1.2.1. LIMITED SLIP SYSTEMS.....	2
1.2.2.TWINNING.....	2
1.2.3.ANISOTROPY.....	3
1.2.4.CREEP RESISTANCE.....	4
1.2.5.CORROSION SUSCEPTIBILITY.....	5
1.3.ALLOYING.....	6
1.3.1.PURPOSE OF ALLOYING.....	6
1.3.1.1.ENHANCING MECANICAL PROPERTIES.....	6
1.3.1.2.IMPROVING CORROSION RESISTANCE.....	6
1.3.1.3.MODIFYING THERMAL PROPERTIES.....	7
1.3.1.4.ENHANCING CASTABILITY AND FORMABILITY...	8
1.3.2.METHODS OF ALLOYING.....	9
1.3.2.1.CASTING.....	9
1.3.2.2.SOLID STATE MIXING.....	9
1.3.2.3.INGOT METALLURGY.....	10
1.3.2.4.INFILTRATION.....	10
1.3.2.5.ELECTROLYTIC METHODS.....	10
1.3.2.6.THERMAL SPRAYING.....	11

1.3.2.7.PLASMA DEPOSITION.....	11
1.3.2.8.DIFFUSION BONDING.....	11
1.3.2.9. LIQUID METAL INFILTRATION.....	12
1.3.2.10.MECHANICAL ALLOYING.....	12
1.3.3. ALLOYING ELEMENTS.....	13
1.3.3.1. PRIMARY ALLOYING ELEMENTS.....	13
1.3.3.1.1. ALUMINIUM.....	13
1.3.3.1.2.ZINC.....	13
1.3.3.1.3.MANGANESE.....	14
1.3.3.2.SECONDARY ALLOYING ELEMENT.....	14
1.3.3.2.1.SILICON.....	14
1.3.3.2.2.BERYLLIUM.....	14
1.3.3.2.3.RARE EARTH ELEMENTS.....	14
1.3.4. TYPES OF MAGNESIUM ALLOYS.....	15
1.3.4.1.AZ (Aluminium Zinc).....	15
1.3.4.2.AM (Aluminium manganese).....	15
1.3.4.3.AE (Aluminium Rare Earth Elements).....	16
1.3.4.4.EZ (Rare Earth Elements Zinc).....	16
1.3.4.5.ZK(Zinc Zirconium).....	16
1.3.4.6.WE(Zirconium Rare Earth Elements).....	16
1.4. Severe Plastic Deformation.....	17
1.4.1. Equal Channel Angular Pressing (ECAP).....	18
1.4.2. High Pressure Torsion(HPT).....	19
1.4.3.Accumulative Roll Bonding(ARB).....	21
1.4.4.High Pressure Sliding(HPS).....	23
1.4.5.Cyclic Extrusion Compression(CEC).....	24
1.4.6.Surface Mechanical Attrition Treatment(SMAT).....	26
1.4.7.Rotary Swaging.....	28

Chapter 2: LITERATURE REVIEW.....	31
Chapter 3: EXPERIMENTATION	
3.1. EQUIPMENT AND SET-UP FOR VACUUM STIR CASTING.....	34
3.1.1.FURNACE.....	34
3.1.2.STIRRING MECHANISM.....	34
3.1.3.CRUCIBLE.....	35
3.1.4.STIRRING TOOLS.....	35
3.1.5.COOLING SETUP.....	35
3.1.6.GAS SUPPLY.....	36
3.1.7. VACUUM CHAMBER.....	36
3.2.MATERIAL SELECTION.....	37
3.3.STIR CASTING PROCEDURE.....	38
3.4.HOT ROLLING OF Mg-Zr-Sn alloy.....	38
3.4.1.EQUIPMENT AND SETUP FOR HOT ROLLING.....	38
3.4.1.1.ROLLING MILL.....	38
3.4.1.2.HEATING FURNACE.....	38
3.4.1.3.ROLL GAP ADJUSTMENT.....	39
3.4.1.4.COOLING SYSTEM.....	39
3.4.1.5.CONVEYORS.....	39
3.4.2.HOT ROLLING PROCEDURE.....	39
3.5.CUTTING AND GRINDING OF STIR CAST Mg-Zr-Sn alloy.....	40
3.5.1.CUTTING.....	40
3.5.2.GRINDING.....	40
3.6.MOUNTING.....	41
3.7.POLISHING.....	41
3.7.1.COARSE GRINDING.....	41

3.7.2.FINE GRINDING.....	42
3.7.3. POLISHING.....	42
3.7.4.FINAL POLISHING.....	42
3.7.5.CLEANING AND INSPECTION.....	43
Chapter 4: MATERIAL CHARACTERISATION	
4.1.ULTIMATE TENSILE TEST.....	44
4.2.SEM-EBSD OBSERVATIONS.....	47
4.3.STEM OBSERVATIONS.....	65
Chapter 5.RESULTS AND DISCUSSION	
5.1. TENSILE TEST ANALYSIS.....	70
5.1.1. ELONGATION (%)......	73
5.1.2.YIELD STRESS.....	73
5.1.3.YIELD RATIO.....	73
5.2. EBSD ANALYSIS.....	75
5.2.1.Mg-0.3% wtZr alloy.....	75
5.2.2.Mg-0.3% wtSn alloy.....	76
5.2.3.Mg-0.3% wtZr-0.3%wtSn alloy.....	76
5.3. STEM analysis.....	78
5.3.1.Mg-0.3% wtZr alloy.....	78
5.3.2.Mg-0.3% wtSn alloy.....	82
5.3.3.Mg-0.3% wtZr-0.3%wtSn alloy.....	84
Chapter 7:CONCLUSION.....	90
Chapter 8: REFERENCES.....	91

LIST OF FIGURES

Fig 1.1: Schematic sketch of Equal Channel Angular Pressing [13].....	18
Fig 1.2: Diagram representing direction of Equal Channel Angular Pressing [14]...19	
Fig 1.3: Schematic diagram of High-Pressure Torsion [12].....	20
Fig 1.4: Sketch representing direction of pressure and rotation in HPT [12].....	21
Fig 1.5: Diagram representing the sequence of Accumulative Roll Bonding [15]....	22
Fig 1.6: Sketch representing the experimental set-up of High-Pressure Sliding [24]..	23
Fig 1.7: Diagram representing the direction of application of pressure in High-Pressure Sliding [24].....	24
Fig 1.8: Diagram representing the experimental set-up of Cyclic Extrusion Compression [21].....	25
Fig 1.9: Diagram representing the direction of application of ram pressure in High-Pressure Sliding[20].....	26
Fig 1.10: Experimental set-up of Mechanical Attrition Treatment [33].....	27
Fig 1.11: Sketch representing the components of Rotary Swaging [28].....	28
Fig 1.12: Diagram representing the direction of application of pressure in Rotary Swaging [28].....	29
Fig 3.1: Experimental set-up of vacuum stir casting equipment.....	37
Fig 3.2: Experimental set-up of Hot Rolling Equipment.....	39
Fig 4.1: Experimental set-up of Ultimate Tensile Test [41].....	44
Fig 4.2: Schematic representation of Scanning Electron Microscope [34].....	47
Fig 4.3: Image describing pump set-up in vacuum system [34].....	49
Fig 4.4: Sketch representing direction of air flow across the pump [34].....	50

Fig 4.5: Diagram representing components of scroll pumps [34].....	50
Fig 4.6: Schematic sketch of gate valve[37].....	52
Fig 4.7: Diagram describing the field emission [34].....	56
Fig 4.8: Diagram describing condenser lens [34].....	57
Fig 4.9: Depiction of various electron scattering [34].....	59
Fig 5.1: Stress-strain plot of Mg-0.3% wtZr alloy.....	70
Fig 5.2: Stress-strain plot of Mg-0.3% wtSn alloy	71
Fig 5.3: Stress-strain plot of Mg-0.3% wtZr-0.3% wtSn alloy.....	71
Fig 5.4: EBSD of sample Mg-0.3% wtZr alloy.....	75
Fig 5.5: EBSD of sample Mg-0.3% wtSn alloy.....	76
Fig 5.6: EBSD of sample Mg-0.3% wtZr-0.3% wtSn alloy.....	76
Fig 5.7: STEM-LAADF, STEM-HAADF and STEM-EDS image of Mg-0.3% wtZr.....	78
Fig 5.8: STEM-LAADF, STEM-HAADF and STEM-EDS image of Mg-0.3% wtSn.....	82
Fig 5.9: STEM-LAADF and STEM-HAADF image of Mg-0.3% wtZr-0.3% wtSn.....	84
Fig 5.10: STEM-EDS image of Mg-0.3% wtZr-0.3% wtSn.....	85

CHAPTER 1

INTRODUCTION

Magnesium, a lightweight and abundant chemical element with an atomic number 12 is the eighth most prevalent element in the earth's crust offering a vast reservoir of potential for various applications. Beyond its fundamental presence in nature, magnesium plays a pivotal role in an array of domains from material science and metallurgy to biological processes and the advancement of sustainable technologies. Its versatility lies in its unique combination of qualities like exceptional low density (about 1.74 g/cm^3), high strength to weight ratio (about 158 KN-m/kg), good thermal conductivity (about 156 W/m-K), good castability, weldability, electromagnetic shielding, excellent damping capacity, dimensional stability, easy recyclability and good bio-compatibility.

1.1. APPLICATIONS OF MAGNESIUM ALLOYS

1.1.1. AUTOMOTIVE INDUSTRY:

In automotive industry, magnesium alloys are primarily employed in engine blocks, cylinder heads, transmission cases, steering components, seat frames, interior components and suspension components [5].

1.1.2. AEROSPACE INDUSTRY:

Magnesium alloys are used in various structural components of aircraft like fuselage frames, wings, landing gear components, seat frames, and overhead compartments and trim panels [5]

1.1.3. MEDICAL SECTOR:

In medical sectors, magnesium alloys are primarily employed in orthopaedic implants, cardiovascular stents and bio-compatible dental implants. [5]

1.1.4. ELECTRONICS INDUSTRY:

In electronics industry, magnesium alloys are primarily employed in laptops, tablets, smartphones, and cameras. While magnesium offers various advantages, it is also susceptible to challenge various limitations like poor formability, poor ductility, corrosion susceptibility and anisotropy. [5]

1.2. LIMITATIONS OF MAGESIUM ALLOYS

The major limitations of magnesium are

1.2.1. LIMITED SLIP SYSTEMS:

Slip systems refer to the specific crystallographic planes and directions along which dislocations move under applied stress, leading to plastic deformation. Magnesium alloys typically exhibit limited slip systems due to their hexagonal close-packed (HCP) crystal structure. In an HCP structure, atoms are densely packed in layers with hexagonal symmetry, and slip occurs predominantly along a limited number of planes and directions, known as the primary slip systems. The limited slip systems in magnesium alloys can result in certain mechanical behaviours that impact their deformation characteristics and mechanical properties. For instance, the limited slip systems may lead to anisotropic deformation behaviour, where the material exhibits different mechanical responses along different crystallographic orientations. This anisotropy can affect the formability, ductility, and texture evolution during deformation processes such as rolling, extrusion, or forging.

Additionally, the limited slip systems can influence the mechanical behaviour of magnesium alloys under various loading conditions. For example, the activation of slip systems may be more restricted in tension-compression asymmetry, where the material exhibits different mechanical responses under tension and compression loading. This can lead to complex deformation behaviour, including tension-compression asymmetry and non-linear stress-strain responses. [5]

1.2.2. TWINNING:

Twinning is another important deformation mechanism in magnesium alloys, alongside dislocation slip. Twinning involves the formation of mirror-image crystallographic domains (twins) in the material, typically along specific crystallographic planes and directions. In magnesium alloys, twinning is particularly prevalent due to the HCP crystal structure, which

promotes easy formation and propagation of twins under certain loading conditions.

Twinning in magnesium alloys can significantly influence their mechanical behaviour, including strength, ductility, and deformation mechanisms. For example, deformation twinning can contribute to the strain hardening and plasticity of magnesium alloys, enhancing their overall strength and work-hardening behaviour. However, excessive twinning may also lead to strain localization, reduced ductility, and susceptibility to premature failure, particularly under complex loading conditions or at elevated temperatures.

The interaction between twinning and slip is another important aspect to consider in the deformation behaviour of magnesium alloys. Twinning can interact with dislocation slip, affecting the overall deformation mechanisms and mechanical properties of the material. Understanding the coupling between twinning and slip is crucial for predicting the mechanical response of magnesium alloys under different loading conditions and developing strategies to optimize their mechanical properties.

1.2.3. ANISOTROPY:

Anisotropy refers to the directional dependence of material properties and mechanical behaviour. In the case of magnesium alloys, anisotropy is primarily attributed to their HCP crystal structure, which results in different mechanical responses along different crystallographic orientations. This anisotropic behaviour can manifest in various mechanical properties, including yield strength, ductility, fracture toughness, and fatigue resistance.

The anisotropic behaviour of magnesium alloys poses challenges in their processing, forming, and utilization in engineering applications. For example, during forming processes such as rolling, extrusion, or forging, the orientation-dependent deformation behaviour can lead to non-uniform strain distribution, texture evolution, and mechanical properties across the material. This can affect the dimensional accuracy, surface finish, and mechanical performance of formed components, necessitating careful consideration of processing parameters and tooling design.

In structural applications, anisotropy can influence the design and performance of magnesium alloy components under different loading conditions. For instance, the orientation-dependent mechanical properties may result in preferential deformation modes, such as twinning or slip, under specific loading directions. This can affect the overall structural integrity, fatigue life, and damage tolerance of components subjected to complex loading environments

1.2.4. CREEP RESISTANCE:

Creep resistance refers to a material's ability to resist deformation under constant load or stress, particularly at elevated temperatures. In magnesium alloys, creep resistance is a significant consideration for applications involving sustained mechanical loading at elevated temperatures, such as high-temperature structural components in aerospace, automotive, and power generation systems.

The creep behaviour of magnesium alloys is influenced by various factors, including microstructure, alloy composition, temperature, and applied stress. Understanding the mechanisms governing creep deformation in magnesium alloys is essential for predicting their long-term performance and designing components with adequate creep resistance.

In magnesium alloy, creep deformation primarily occurs through dislocation glide and climb mechanisms, facilitated by diffusion processes at elevated temperatures. The rate of creep deformation is governed by parameters such as the applied stress, temperature, grain size, and the presence of strengthening precipitates or phases.

Magnesium alloys typically exhibit limited creep resistance compared to some other engineering materials like aluminium alloys or nickel-based super alloys. This is primarily attributed to their hexagonal close-packed crystal structure, which leads to limited slip systems and higher dislocation mobility at elevated temperatures.

To improve the creep resistance of magnesium alloys, various alloying elements, microstructural modifications, and processing techniques are employed. Alloying elements such as aluminium, zinc, and rare earth

metals can form strengthening precipitates or solid solution strengthening phases, which inhibit dislocation movement and retard creep deformation. Additionally, grain refinement techniques, including severe plastic deformation and grain boundary engineering, can enhance the creep resistance by minimizing grain boundary sliding and enhancing grain boundary pinning effects. [5]

1.2.5. CORROSION SUSCEPTIBILITY:

Corrosion susceptibility is a significant limitation of magnesium alloys, particularly in environments containing moisture, saltwater, acids, or other corrosive agents. Despite their attractive mechanical properties, magnesium alloys are prone to corrosion due to their electrochemical reactivity and the formation of corrosion products on their surface.

The corrosion behaviour of magnesium alloys is influenced by various factors, including alloy composition, microstructure, surface condition, environmental exposure, and service conditions. Magnesium alloys can undergo different types of corrosion, including uniform corrosion, pitting corrosion, galvanic corrosion, and stress corrosion cracking (SCC), depending on the specific conditions and mechanisms involved.

Uniform corrosion involves the relatively uniform dissolution of the metal surface, leading to a loss of material and degradation of mechanical properties over time. Pitting corrosion is characterized by localized attack and the formation of pits or cavities on the metal surface, which can penetrate deeply into the material and compromise structural integrity.

Galvanic corrosion occurs when magnesium alloys are in contact with dissimilar metals in an electrolyte, leading to accelerated corrosion of the magnesium component due to galvanic coupling. This can occur in mixed-metal assemblies or in environments where magnesium alloys are coupled with more noble metals such as stainless steel or aluminium.

Stress corrosion cracking (SCC) is another critical corrosion mechanism that can occur in magnesium alloys under tensile stress in the presence of corrosive environments. SCC is a type of environmentally assisted cracking

that can lead to sudden and catastrophic failure of magnesium alloy components, particularly in aerospace, automotive, and marine applications. In order to overcome the limitations the primary methods carried out is alloying and Severe Plastic Deformation (SPD) techniques. It helps in grain size reduction, texture modification through weakening and randomisation (rotation of grains from basal orientation to non-basal orientation), reducing the CRSS difference between planes and reducing the c/a ratio thus ensuring better formability and ductility. [5]

1.3. ALLOYING

Alloying involves combination of two or more metallic elements to create a new material with improved properties. The selection of alloying elements determines the final properties of the magnesium alloy. Several factors influence the choice of alloying elements

1.3.1. PURPOSE OF ALLOYING

The intended application of magnesium alloy plays a significant role in selecting the alloying elements.

1.3.1.1. ENHANCING MECHANICAL PROPERTIES

Pure magnesium, while lightweight, lacks the mechanical strength required for many structural applications. Alloying elements are added to improve strength, hardness, and other mechanical properties. Common alloying elements include aluminium, zinc, manganese, and rare earth elements such as cerium and zirconium. These elements form solid solutions or intermetallic compounds within the magnesium matrix, imparting strength through mechanisms like solid solution strengthening, precipitation hardening, and grain refinement. [5]

1.3.1.2. IMPROVING CORROSION RESISTANCE

Magnesium alloys are susceptible to corrosion in various environments, including moisture, saltwater, acids, and alkaline solutions. Alloying is employed to enhance the corrosion resistance of magnesium alloys by

forming protective oxide layers, corrosion-resistant phases, or sacrificial elements. This is crucial for expanding the applicability of magnesium alloys in corrosive environments and increasing their service life. Alloying elements such as aluminium, zinc, and manganese promote the formation of stable oxide layers (e.g., MgO, Al₂O₃, ZnO) on the surface of magnesium alloys, acting as barriers against corrosive agents. These oxide layers inhibit further corrosion by limiting the diffusion of corrosive species and protecting the underlying substrate. Certain alloying elements can precipitate as corrosion-resistant phases within the magnesium matrix, enhancing the material's resistance to localized corrosion, pitting corrosion, and stress corrosion cracking (SCC). Rare earth metals, zinc, and manganese are known for their ability to improve the corrosion resistance of magnesium alloys through the formation of protective phases. Alloying elements with higher electrochemical potential than magnesium, such as zinc and aluminium, can act as sacrificial anodes within magnesium alloys, corroding preferentially to protect the magnesium substrate. Sacrificial anodes are commonly used in marine applications to prevent galvanic corrosion of magnesium components in contact with seawater. [5]

1.3.1.3. MODIFYING THERMAL PROPERTIES

Alloying elements can influence the thermal properties of magnesium alloys, including thermal conductivity, coefficient of thermal expansion (CTE), and melting temperature. These properties are critical for applications requiring thermal management, dimensional stability, and compatibility with joining processes such as welding, brazing, and soldering. Alloying elements may enhance or diminish the thermal conductivity of magnesium alloys, depending on their composition, microstructure, and interactions with phonon scattering mechanisms. For instance, aluminium and zinc alloying elements tend to decrease the thermal conductivity of magnesium alloys due to their higher atomic mass and phonon scattering effects. Alloying elements can alter the CTE of magnesium alloys, influencing their dimensional stability, compatibility with dissimilar materials, and susceptibility to thermal stress. The addition

of aluminium, zinc, or rare earth metals may adjust the CTE of magnesium alloys to match that of surrounding materials in multi-material assemblies or thermal management applications. Certain alloying elements may raise or lower the melting temperature of magnesium alloys, affecting their process ability, casting behaviour, and solidification characteristics. Alloying elements such as aluminium and rare earth metals can increase the melting temperature of magnesium alloys, improving their high-temperature performance and creep resistance. [5].

1.3.1.4. ENHANCING CASTABILITY AND FORMABILITY

Alloying plays a crucial role in enhancing the castability and formability of magnesium alloys, enabling the production of complex shapes, thin-walled components, and intricate geometries through various casting, forming, and fabrication processes. Alloying elements influence the fluidity, solidification behaviour, hot workability, and microstructural evolution of magnesium alloys during processing. Alloying elements such as aluminium, manganese, and zinc improve the fluidity and castability of magnesium alloys by reducing the tendency for hot tearing, shrinkage defects, and microstructural segregation during casting processes. These elements promote uniform solidification, finer grain structures, and smoother surface finishes in cast magnesium components. Certain alloying elements enhance the hot workability and formability of magnesium alloys by reducing the flow stress, improving the ductility, and facilitating dynamic recrystallization during hot deformation processes such as extrusion, forging, and rolling. Aluminium, zinc, and rare earth metals contribute to the improvement of formability and process ability in wrought magnesium alloys. Alloying elements can influence the machinability of magnesium alloys, affecting chip formation, tool wear, surface finish, and dimensional accuracy during machining operations such as turning, milling, and drilling. Additions of lead, bismuth, or sulphur may improve the machinability of magnesium alloys by promoting chip breakage and reducing cutting forces.

The process of alloying magnesium involves several methods, each with its advantages and limitations. These methods are used to create the desired chemical composition and microstructure in the alloy. [5]

1.3.2. METHODS OF ALLOYING

Commonly used methods include,

1.3.2.1. CASTING

Casting is a widely employed method for alloying magnesium due to its simplicity and versatility. This process involves melting magnesium along with other alloying elements, such as aluminium, zinc, or rare earth metals, and then pouring the molten alloy into moulds to form desired shapes and structures. The molten alloy solidifies within the moulds, retaining the composition of the alloying elements. Casting offers several advantages, including the ability to produce complex shapes, cost-effectiveness in mass production, and suitability for large-scale manufacturing. However, casting may lead to porosity and other defects in the final product, requiring additional processing steps for quality assurance. [1]

1.3.2.2. SOLID STATE MIXING

Solid-state mixing encompasses various mechanical methods of blending magnesium with alloying elements in their solid forms. Techniques such as ball milling and powder metallurgy are commonly employed to achieve uniform distribution of alloying elements within the magnesium matrix. Ball milling involves the grinding of magnesium and alloying powders together in a rotating drum, facilitating the intimate mixing of particles at the micro scale. Powder metallurgy utilizes pressing and sintering of magnesium and alloying powders to form dense compacts, which are then subjected to heat treatment to promote diffusion and alloy formation. Solid-state mixing offers precise control over alloy composition and microstructure, making it suitable for producing high-performance magnesium alloys with tailored properties. [1]

1.3.2.3.INGOT METALLURGY

Ingot metallurgy involves the melting of pure magnesium along with alloying elements to form homogeneous melts, which are then solidified into ingots through casting or other shaping processes. The ingots can be further processed through hot or cold working techniques to fabricate components with specific geometries and properties. Ingot metallurgy allows for the production of bulk quantities of magnesium alloys with controlled compositions and uniform microstructures. However, the process may lead to segregation of alloying elements and formation of undesirable phases, necessitating careful optimization of processing parameters.[1]

1.3.2.4.INFILTRATION

Infiltration techniques enable the introduction of alloying elements into a porous magnesium matrix by impregnating the matrix with a molten alloy. This method is particularly suited for producing composite materials with enhanced mechanical, thermal, or electrical properties. In liquid metal infiltration, molten alloys containing desired elements are infiltrated into preforms or porous substrates made of magnesium or other materials. The molten alloy fills the void spaces within the substrate, resulting in a composite structure with a homogeneous distribution of alloying elements. Infiltration techniques offer flexibility in designing composite materials with tailored compositions and properties, making them suitable for various applications in aerospace, automotive, and electronics industries.[1]

1.3.2.5.ELECTROLYTIC METHODS

Electrolytic processes can be employed to deposit alloying elements onto a magnesium substrate, thereby modifying its surface composition and properties. Electroplating involves the electrode position of alloying metals or compounds from an electrolyte solution onto a cathodic magnesium substrate. The electrolyte solution contains dissolved ions of the alloying elements, which are reduced at the cathode surface to form a metallic coating. Electrolytic methods offer precise control over coating thickness and composition, enabling the fabrication of corrosion-resistant, wear-

resistant, or decorative finishes on magnesium components. However, electrolytic processes may involve complex equipment and require careful control of operating parameters to achieve desired coating properties.

1.3.2.6. THERMAL SPRAYING

Thermal spraying techniques involve the deposition of alloying materials onto a magnesium surface in the form of fine particles or droplets. In thermal spray processes such as flame spraying, arc spraying, and plasma spraying, alloying powders are heated to high temperatures and propelled onto the substrate using a gas or plasma jet. Upon impact, the particles form a coating layer on the magnesium surface, bonding mechanically and metallurgically with the substrate. Thermal spraying offers advantages such as fast deposition rates, minimal substrate heating, and suitability for coating large and complex geometries. The resulting coatings exhibit improved wear resistance, thermal insulation, or electrical conductivity, depending on the composition of the alloying materials. [1]

1.3.2.7. PLASMA DEPOSITION

Plasma deposition is a specialized technique for depositing thin films of alloying materials onto a magnesium substrate using a plasma-enhanced chemical vapour deposition (PECVD) process. In PECVD, precursor gases containing alloying elements are introduced into a vacuum chamber, where they are ionized into a plasma state by radiofrequency or microwave energy. The activated species in the plasma react with the magnesium surface, forming a thin film of the alloy through chemical reactions and deposition processes. Plasma deposition offers precise control over film thickness, composition, and microstructure, enabling the fabrication of functional coatings with specific optical, electrical, or barrier properties. However, plasma deposition systems can be complex and expensive, requiring skilled operation and maintenance. [1]

1.3.2.8. DIFFUSION BONDING

Diffusion bonding is a solid-state joining process that facilitates the formation of alloyed interfaces between magnesium components containing

different alloying elements. In diffusion bonding, the mating surfaces of magnesium components are brought into intimate contact under controlled pressure and temperature conditions. At elevated temperatures, the alloying elements diffuse across the interface, leading to the formation of a diffusion zone with a composition intermediate between the parent materials. Diffusion bonding enables the fabrication of multi-material structures with tailored properties and functionalities, such as dissimilar metal joints, laminated composites, and gradient alloys. However, diffusion bonding requires precise control of bonding parameters and may involve long processing times for achieving adequate diffusion depths. [1]

1.3.2.9. LIQUID METAL INFILTRATION

Liquid metal infiltration techniques involve impregnating a porous magnesium matrix with molten alloys containing desired alloying elements. In squeeze casting, the molten alloy is forced into the interstices of a preform or porous substrate under high pressure, ensuring complete infiltration and consolidation of the composite material. Liquid metal infiltration enables the fabrication of magnesium-based composites with enhanced mechanical, thermal, or electromagnetic properties, suitable for applications requiring lightweight and high-performance materials. However, liquid metal infiltration processes may be limited by the availability of suitable preforms and the challenges associated with controlling alloy flow and solidification behaviour. [1]

1.3.2.10. MECHANICAL ALLOYING

Mechanical alloying is a solid-state powder processing technique used to synthesize homogeneous alloys by repeated cold welding, fracturing, and rewelding of powder particles. In mechanical alloying, elemental powders of magnesium and alloying elements are mixed together in a high-energy ball mill, where the kinetic energy of the milling media promotes intimate mixing and alloy formation through solid-state diffusion and deformation processes. Mechanical alloying enables the production of Nano-crystalline or amorphous alloys with unique mechanical, thermal, and magnetic properties, offering

advantages such as fine microstructure control, enhanced solid solubility, and improved mechanical properties. However, mechanical alloying requires careful selection of milling parameters, milling media, and protective atmospheres to prevent contamination and ensure reproducible results.

The alloying elements are categorised into primary and secondary groups, each serving distinct roles in modifying the properties of magnesium alloys [5]. Primary alloying elements are added in higher concentrations and play a more prominent role in determining the alloy's properties while the secondary alloying elements are used in smaller quantities to refine specific properties.

1.3.3. ALLOYING ELEMENTS

1.3.3.1. PRIMARY ALLOYING ELEMENTS

The commonly used primary alloying elements are

1.3.3.1.1. ALUMINIUM

The addition of aluminium enhances the strength and ductility of magnesium alloys. The primary strengthening mechanisms of aluminium in magnesium alloys are solid solution strengthening and precipitation hardening. In solid solution strengthening aluminium dissolves in the magnesium matrix, forming solid solution whose interaction improves the alloy's mechanical properties by impeding dislocation motion. In precipitation hardening, the formation of fine precipitates during heat treatment further increases the strength of the alloy.

1.3.3.1.2. ZINC

Zinc as an alloying element to magnesium provides additional means of solid solution strengthening and enhances the alloy's strength, corrosion resistance and castability. The combination of aluminium and zinc in magnesium alloys is a common practice to achieve a balance of strength and ductility.

1.3.3.1.3. MANGANESE

Manganese as a primary alloying element improves both strength through solid solution strengthening and castability through the modification of microstructure [2].

1.3.3.2. SECONDARY ALLOYING ELEMENTS

The commonly used secondary alloying elements are

1.3.3.2.1. SILICON

Silicon as an alloying element in magnesium enhances the castability and improves the thermal conductivity.

1.3.3.2.2. BERYLLIUM

Beryllium as a secondary alloying element improves specific properties such as electrical conductivity and corrosion resistance. However the use of beryllium is limited due to its toxicity and its concentration in alloys is closely regulated.

1.3.3.2.3. RARE EARTH ELEMENTS

In recent years the most widely used alloying elements in magnesium for the improvement in its properties are rare-earth elements. Rare-earth elements are group of seventeen chemically similar elements found in the lanthanide series of the periodic table along with scandium and yttrium which are often considered part of this group due to their similar properties. The on-going research into the application of rare-earth elements as alloying agents in magnesium not only addresses the limitations of pure magnesium but also contributes to the development of lightweight, high performance materials with improved properties and enhanced corrosion resistance.

However there are various limitations and challenges associated with rare-earth elements along with its advantages. One of the primary drawbacks of rare earth elements is their uneven global distribution with China

dominating the production of these elements, raising concerns about supply chain vulnerabilities and potential geopolitical tensions. This concentration of production can lead to price fluctuations and supply shortages affecting industries heavily reliant of rare earth elements. Another major limitation is the environmental impact associated with its mining and processing. Extracting rare earth elements involves complex, energy intensive procedures often result in extensive environmental degradation and the generation of hazardous waste products, posing risks to human health and ecosystem. Also due to their similar chemical properties, the separation process is arduous and necessitates highly specialized techniques, increasing the overall cost and environmental impact of its production [10].

Thus it is important to develop magnesium alloys using rare-earth free elements to overcome the difficulties of rare earth elements and to obtain the desired properties in an economically viable manner.

1.3.4. TYPES OF MAGNESIUM ALLOYS

The major types of magnesium alloys are

1.3.4.1.AZ (Aluminium Zinc)

COMPOSITION:

Aluminium (Al) - 5% to 9%

Zinc (Zn) – 0.4% to 1 %

Manganese (Mn) – up to 0.15%

Zirconium (Zr) – up to 0.1%

AZ alloys are known for their excellent strengths, corrosion resistance and castability.

1.3.4.2.AM (Aluminium Manganese)

COMPOSITION:

Aluminium (Al) – 0.5% to 5%

Manganese (Mn)- 0.2% to 1.5%

Zinc (Zn) and Zirconium (Zr) - in trace amounts

AM alloys are well regarded for their excellent castability and good ductility.

1.3.4.3.AE (Aluminium Rare-Earth Elements)

COMPOSITION:

Aluminium (Al) – 5% to 10%

Rare Earth Elements (REEs) – 2% to 5%

Zinc (Zn) and Zirconium (Zr) - in trace amounts

AE alloys are known for their high temperature performance and corrosion resistance.

1.3.4.4.EZ (Rare-Earth Elements Zinc)

COMPOSITION:

Rare Earth Elements (REEs) – 2% to 5%

Zinc (Zn) – 1% to 3%

Aluminium and Zirconium- in trace amounts

EZ alloys are well regarded for its high temperature performance and creep resistance.

1.3.4.5.ZK (Zinc Zirconium)

COMPOSITION:

Zinc (Zn) – 3% to 7%

Zirconium (Zr) – 0.4% to 1%

ZK alloys are known for its high strength and corrosion resistance capabilities.

1.3.4.6.WE (Zirconium Rare-Earth Elements)

COMPOSITION:

Zirconium (Zr) - 1% to 3%

Rare Earth Elements (REEs) – 2% to 5%

WE alloys are well regarded for its high temperature performance and creep resistance [5].

1.4. SEVERE PLASTIC DEFORMATION

Severe plastic deformation is a specialised and highly effective material processing technique used to significantly enhance the mechanical properties and microstructure of metals. It involves subjecting a material to an extremely high level of plastic deformation under controlled conditions, typically at room temperature or slightly elevated temperatures, to induce remarkable changes in its structure and properties. The primary purpose of severe plastic deformation is to achieve grain refinement and enhancement of mechanical properties.

Grain refinement involves significant reduction in average grain size. The grain size reduction occurs as a result of intense shear forces and dislocation motion imposed by the deformation process. Smaller grain size is highly desirable as they enhance the material's strength, hardness, and wear resistance. The increased grain boundaries also inhibit dislocation motion, resulting in improved mechanical properties. Furthermore, a finer microstructure can lead to improved ductility and fracture toughness.

Enhancement of mechanical properties involves increase in material's strength, hardness, and fatigue resistance while improving its resistance to wear and corrosion. These property improvements arise from a combination of factors, including grain refinement, the formation of high-angle grain boundaries, and the introduction of residual strains. Additionally, the resulting microstructure often exhibits increased thermal stability which is beneficial for high-temperature applications [11].

The major types of Severe Plastic Deformation (SPD) techniques are

1.4.1. Equal Channel Angular Pressing (ECAP)

The principle of ECAP revolves around severe plastic deformation through repetitive straining. The deformation occurs in a controlled manner within an angular channel, which imparts significant strain to the material without causing fracture. The main components of an ECAP include a die consisting of two intersecting channels, typically at 90-degree angle and a press for applying compressive force.

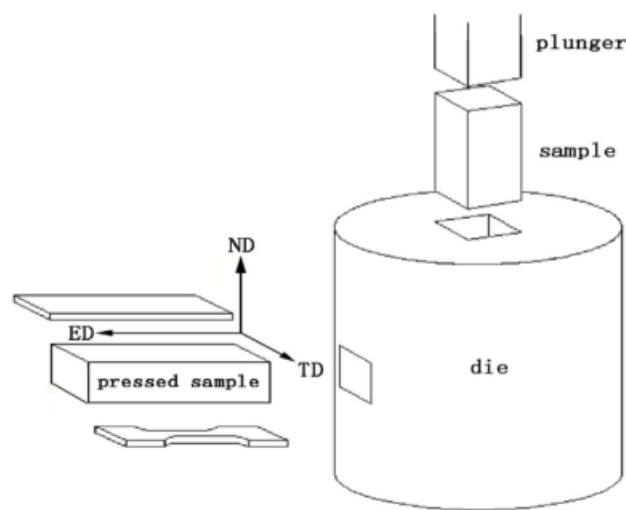


Fig1.1: Schematic sketch of Equal Channel Angular Pressing [13]

The process begins with the preparation of a cylindrical billet of required alloy. The die is designed with two channels intersecting at right angles. The angle of intersection determines the amount of strain imparted to the material. In some cases, the billet can be heated to facilitate plastic deformation and reduce flow stress of the material. The heated or unheated billet is then placed in the die and a hydraulic or mechanical press applies a compressive force to push the billet through the channels. To achieve significant grain refinement, the billet may undergo multiple passes through the die, with the orientation of the billet being adjusted after each pass. After ECAP processing, the material is taken for further heat treatment or mechanical processing to enhance its properties or to achieve specific microstructural characteristics. The microstructural evolution during ECAP involves several mechanisms including grain fragmentation (initial coarse

grains are fragmented into smaller grains due to accumulation of dislocations and formation of new grain boundaries), Grain boundary migration and dynamic recrystallization (where new grains nucleate and grow within the deformed matrix further refining the microstructure). The major advantages of ECAP include grain refinement, homogeneity, complex shapes and optimal cost. [13].

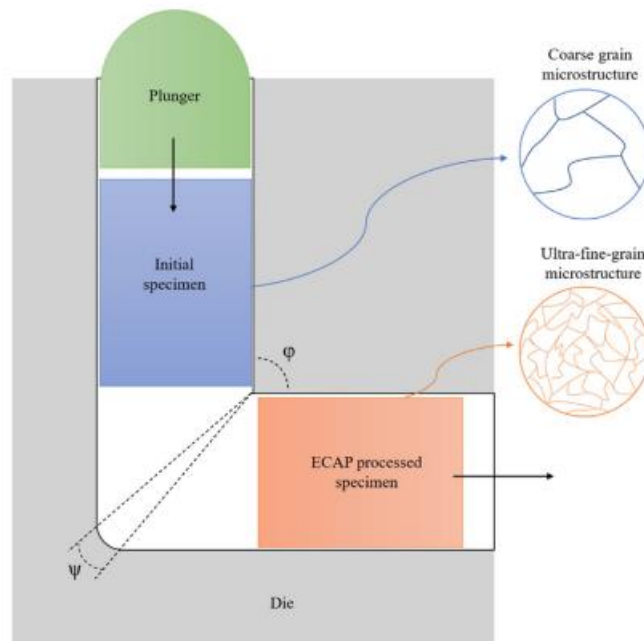


Fig1.2. Diagram representing direction of Equal Channel Angular Pressing [14]

1.4.2. High-Pressure Torsion (HPT)

High Pressure Torsion (HPT) is a solid-state processing technique used to refine the microstructure and improve the mechanical properties of materials, particularly metals and alloys. This method applies a combination of high pressure and torsional deformation to the material, leading to significant grain refinement and modification of its properties. The fundamental principle behind HPT involves subjecting a small specimen of the material to simultaneous application of high pressure and torsional deformation. This is typically achieved using a specialized HPT apparatus, which consists of a chamber capable of generating high pressures and a mechanism for applying torsional deformation to the sample.

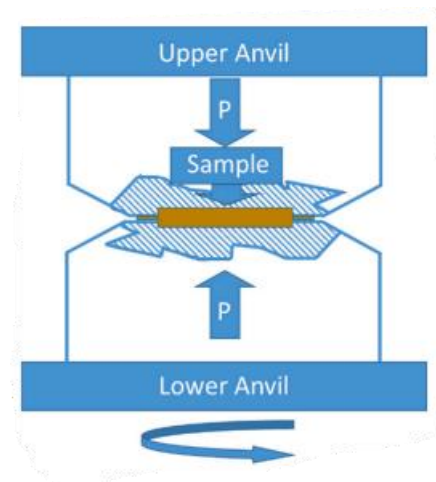


Fig.1.3: Schematic diagram of High-Pressure Torsion [27]

The HPT process begins with the preparation of a cylindrical sample of the material to be processed. The sample is usually cut from a larger piece and machined to the desired dimensions. Prior to deformation, the sample may undergo pre-treatments such as annealing to remove any pre-existing defects or impurities and to facilitate uniform deformation during the HPT process. Once the sample is prepared, it is loaded into the HPT chamber and subjected to high pressure while simultaneously being subjected to torsional deformation. The pressure is typically applied using a hydraulic system, which can generate pressures ranging from a few hundred megapascals to several gigapascals. The torsional deformation is applied using a specialized tool, such as a torsion disc or anvils, which exerts a twisting force on the sample. During the HPT process, the combination of high pressure and torsional deformation causes the material to undergo severe plastic deformation. This leads to the generation of high densities of dislocations and deformation twins within the material, as well as significant grain refinement. The high pressure helps to suppress the formation of new grains and promote the formation of a highly uniform ultrafine-grained microstructure.

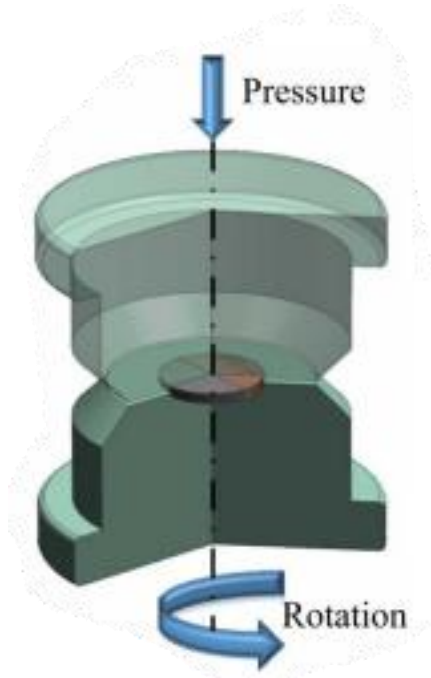


Fig1.4: Sketch representing direction of pressure and rotation in HPT [26]

The microstructural evolution during HPT can be described in several stages. In the initial stages of deformation, dislocations and deformation twins begin to nucleate and propagate within the material, leading to the formation of sub grains. As deformation continues, these sub grains further deform and rearrange, ultimately leading to the formation of ultrafine grains with sizes on the order of tens to hundreds of nanometres. The resulting ultrafine-grained microstructure has several beneficial properties compared to conventional coarse-grained materials. One of the most significant advantages is the dramatic increase in strength and hardness, which can be several times higher than that of the original material. This is due to the high density of grain boundaries and the presence of dislocations, which act as barriers to dislocation motion and strengthen the material. The major advantage of HPT includes grain refinement, improved mechanical properties, homogeneous microstructure and enhanced mechanical performance. [25]

1.4.3. Accumulative Roll Bonding (ARB)

Accumulative Roll Bonding (ARB) is a severe plastic deformation (SPD) process utilized for refining grain structures in metallic materials.

ARB specifically involves repeatedly stacking and rolling thin metal sheets to achieve high strain levels, resulting in ultrafine-grained (UFG) or nanostructured materials. The fundamental principle of ARB revolves around the application of large strains to metallic materials through rolling. The process begins with

stacking multiple thin metal sheets, typically of the same or different materials, to form a composite

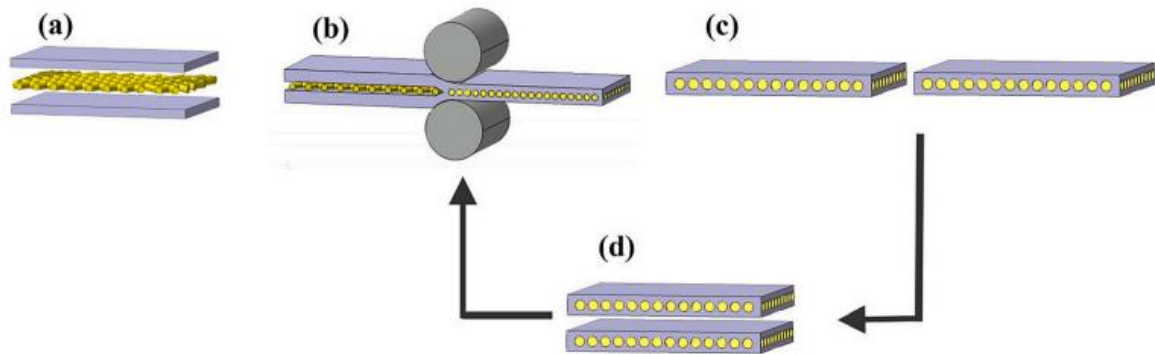


Fig1.5: Diagram representing the sequence of Accumulative Roll Bonding [15] billet. This billet is then subjected to high-pressure rolling, where it undergoes plastic deformation. After each rolling pass, the billet is cut into halves or quarters, and the resulting layers are stacked again to repeat the process. Through multiple cycles of stacking and rolling, the material undergoes cumulative plastic deformation, leading to grain refinement and the formation of ultrafine-grained microstructures.

ARB achieves grain refinement through Severe Plastic Deformation (The repeated rolling and stacking cycles subject the material to severe plastic deformation, leading to the fragmentation and subdivision of grains into smaller sizes), Dynamic Recrystallization (The high strain rates and temperatures during rolling promote dynamic recrystallization, where new grains nucleate and grow within the deformed matrix, resulting in a refined microstructure), Grain Boundary Sliding (The sliding motion of grain boundaries during rolling facilitates grain refinement by redistributing strain and promoting the formation of new grain boundaries) and Dislocation Accumulation and Interaction (The accumulation and interaction of dislocations within the material contribute to grain refinement by promoting the formation of low-angle grain boundaries and inhibiting grain growth.). The advantages of ARB include Grain Refinement, Uniformity, flexibility (wide range of materials) and scalability (can be scaled up for mass production) [14].

1.4.4. High-Pressure sliding (HPS)

The high-pressure sliding (HPS) technique involves subjecting a sample material to a combination of high pressure and shear strain. The basic principle involves applying pressure while simultaneously sliding or rotating the sample, typically between two anvils or discs. This process induces severe plastic deformation within the material, resulting in grain refinement and improved mechanical properties.

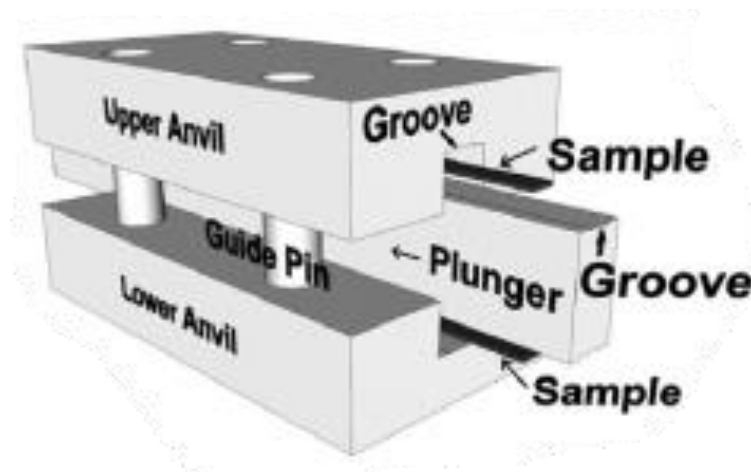


Fig1.6: Sketch representing the experimental set-up of High-Pressure Sliding [24]

The material to be processed is typically prepared in the form of a disk or cylinder. The sample is placed between two anvils or discs within the HPS apparatus. High pressure is applied to the sample using a hydraulic press, mechanical press, or specialized equipment capable of generating the required pressure. While under pressure, the sample is subjected to shear or sliding motion between the anvils or discs. This motion induces plastic deformation within the material. The combination of high pressure and shear strain leads to the deformation of the material, causing grain refinement and structural changes. After the desired deformation is achieved, the pressure is released and the deformed sample is removed from the apparatus for further analysis or processing.

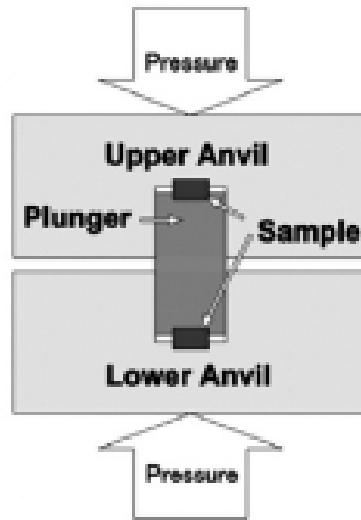


Fig1.7: Diagram representing the direction of application of pressure in High-Pressure Sliding [24]

The mechanism observed in HPS technique includes grain boundary sliding, dislocation generation and accumulation, dynamic recovery and recrystallization and grain boundary migration. [24]

1.4.5. Cyclic Extrusion Compression (CEC)

Cyclic Extrusion Compression (CEC) is a specialized SPD technique that combines extrusion and compression processes in a cyclic manner. The primary objective of CEC is to refine the grain structure of materials through repetitive deformation cycles. The cyclic nature of CEC distinguishes it from conventional extrusion or compression techniques, allowing for enhanced grain refinement and mechanical property improvements. The principles underlying CEC involve subjecting the material to alternating compression and extrusion cycles. During compression, the material experiences high pressure, causing plastic deformation and grain refinement. Subsequent extrusion relieves the accumulated strain and further refines the grain structure. The repetitive application of compression and extrusion cycles facilitates the formation of ultrafine grains, leading to superior mechanical properties.

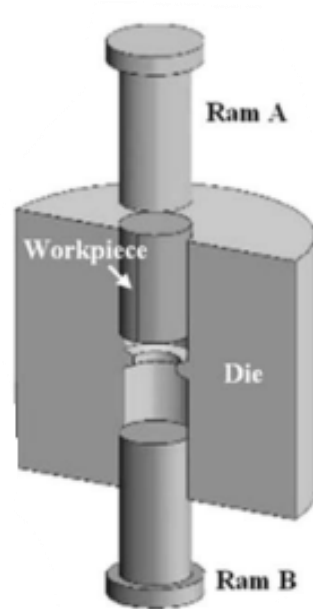


Fig1.8: Diagram representing the experimental set-up of Cyclic Extrusion Compression [21]

The CEC process involves preparing the material in the form of a billet or rod followed by heating to an elevated temperature to facilitate plastic deformation and reduce the flow stress of the material. The heated billet is subjected to high compressive forces leading to plastic deformation and grain refinement. Following compression, the material undergoes extrusion to relieve the accumulated strain and further refine the grain structure. The compression and extrusion steps are repeated cyclically to achieve the desired grain size and mechanical properties. After completing the CEC cycles, the material undergoes additional processing such as annealing or heat treatment to optimize its properties. The mechanisms of grain refinement in CEC include Dislocation Accumulation and sub-grain formation, dynamic recrystallization and grain boundary sliding and rotation.[21]

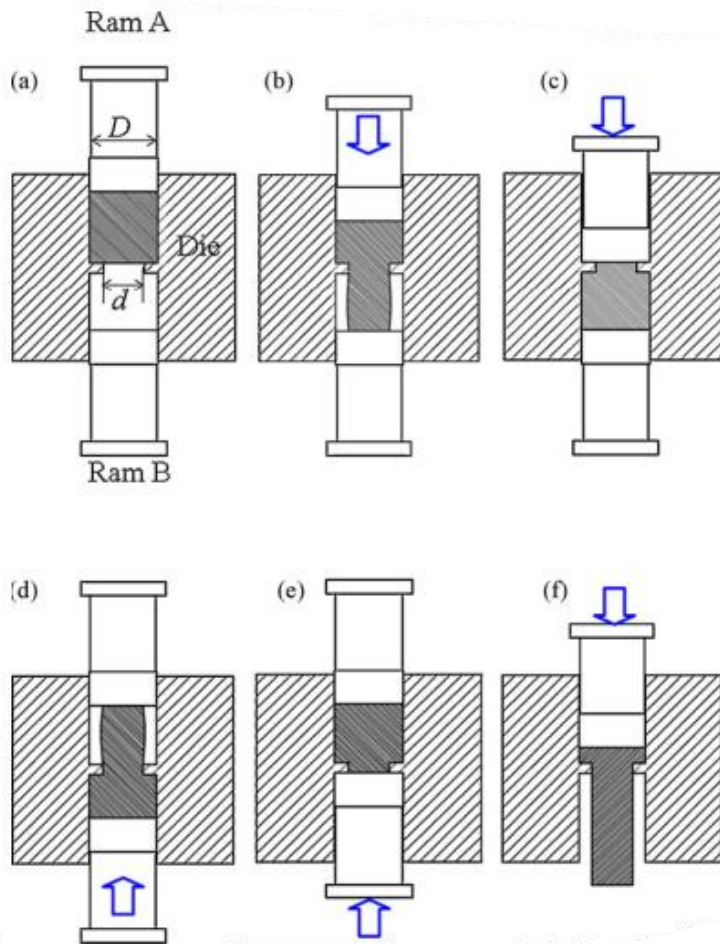


Fig1.9: Diagram representing the direction of application of ram pressure in High-Pressure Sliding [20]

1.4.6. Mechanical Attrition Treatment

The principle behind mechanical attrition treatment is to apply mechanical stress to materials to break them down into smaller particles or induce structural changes. By subjecting materials to intense mechanical forces, it is possible to alter their morphology, particle size distribution, surface area, and crystallinity. Mechanical attrition treatment can be carried out using various types of equipment, including ball mills, attritors, planetary mills, and vibratory mills. These machines apply mechanical energy to the material through collisions between the grinding media (balls or beads) and the material being processed.

The process typically involves placing the material to be treated along with grinding media in a container or chamber. The container is then rotated, vibrated, or subjected to other mechanical motions to cause the grinding media to impact and shear the material. One of the primary objectives of mechanical attrition treatment is to reduce the particle size of the material. As the grinding media collide with the material, they break it down into smaller particles through a combination of impact, compression, and shear forces. This reduction in particle size leads to an increase in the specific surface area of the material, which can enhance its reactivity or improve properties such as strength and conductivity. In addition to particle size reduction, mechanical attrition treatment can also induce structural modifications in the material.

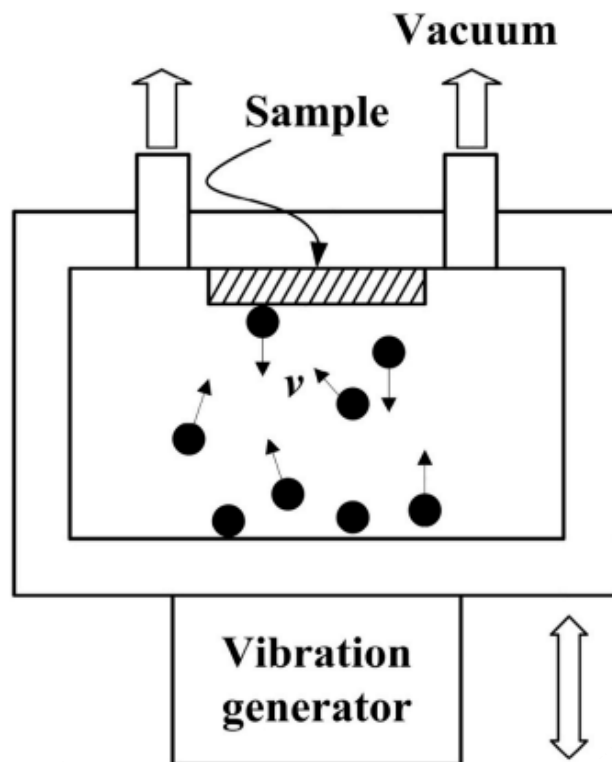


Fig 1.10: Experimental set-up of Mechanical Attrition Treatment [33]

The high-energy collisions between the grinding media and the material can cause dislocations, defects, and rearrangements of atoms or molecules within the material's crystal lattice. These structural changes can alter the material's mechanical, electrical, magnetic, or optical properties.

The effectiveness of mechanical attrition treatment depends on several parameters, including the type and size of grinding media, the speed and duration of milling,

the material's properties, and the presence of any additives or surfactants. Controlling these parameters allows researchers to tailor the treatment process to achieve specific desired outcomes. Mechanical attrition treatment finds applications in various fields, including nanoparticle synthesis, composite materials fabrication, powder metallurgy, pharmaceuticals, and ceramics. For example, in the production of nanoparticles, mechanical attrition treatment can be used to produce uniform nanoparticles with controlled size and morphology. Mechanical attrition treatment offers several advantages, such as scalability, simplicity, and the ability to process a wide range of materials. However, it may also have limitations, including the generation of heat, contamination from the grinding media, and the potential for non-uniform particle size distribution. [33]

1.4.7. Rotary Swaging

Rotary swaging is a metal forming process used to shape cylindrical work pieces through severe plastic deformation. This technique involves the application of compressive forces to the work piece while it is rotated and displaced between a set of rotating dies. Rotary swaging is particularly effective for producing complex geometries, reducing the diameter of cylindrical components, and improving material properties such as strength and hardness.

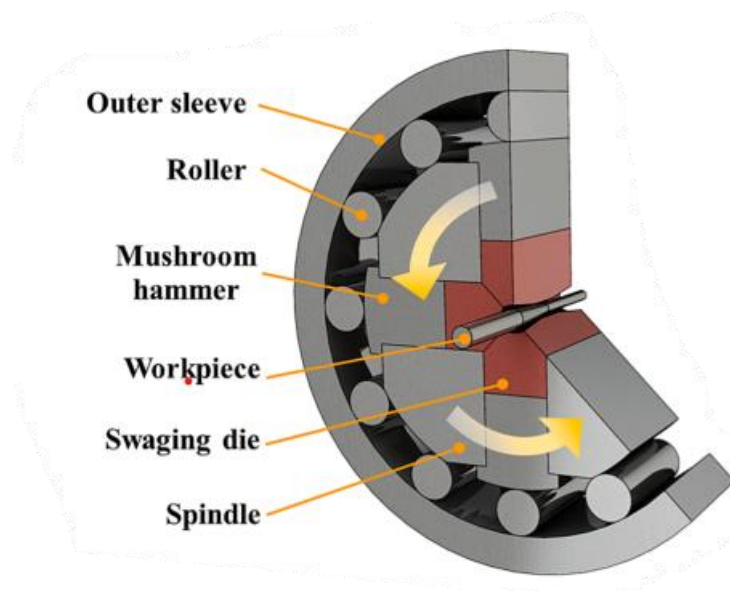


Fig1.11: Sketch representing the components of Rotary Swaging [28]

The fundamental principle of rotary swaging involves the controlled reduction of the diameter of a cylindrical work piece through the application of radial compressive

forces. This process is achieved by rotating the work piece and simultaneously feeding it through a series of rotating dies. The dies exert pressure on the work piece, causing it to deform plastically and flow into the desired shape. [29].

Rotary swaging operates on several deformation mechanisms, including axial compression, radial expansion, torsion, and bending. These mechanisms work together to reshape the work piece, resulting in a reduction in diameter and an increase in length. The precise combination of these deformation modes depends on factors such as the design of the dies, the material properties of the work piece, and the process parameters. Rotary swaging machines consist of several key components, including the main spindle, rotating dies, feed mechanism, and control system. The main spindle provides rotational motion to the work piece, while the rotating dies apply radial pressure to deform the work piece.

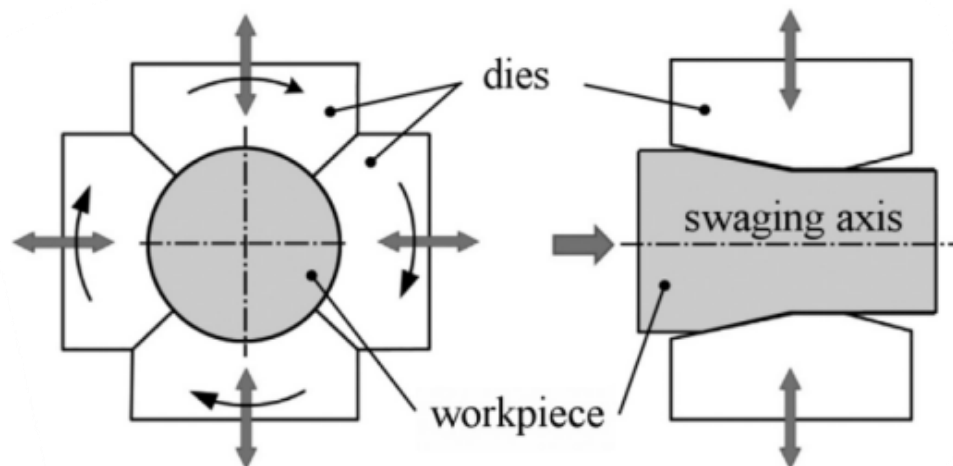


Fig 1.12:

Diagram representing the direction of application of pressure in Rotary Swaging [29]

The feed mechanism controls the rate at which the work piece is fed through the dies, allowing for precise control over the deformation process. The control system monitors and adjusts various parameters such as force, speed, and temperature to optimize the swaging process.

During rotary swaging, the microstructure of the work piece undergoes significant changes as a result of the severe plastic deformation. Grain refinement, dislocation generation, and texture development are common features of rotary-swaged

materials. The precise microstructural evolution depends on factors such as the material composition, deformation conditions, and processing parameters. Rotary-swaged materials typically exhibit improved mechanical properties compared to their pre-swaged counterparts. The severe plastic deformation induces grain refinement and work hardening, resulting in enhanced strength, hardness, and fatigue resistance. Additionally, the texture development in rotary-swaged materials can lead to anisotropic mechanical properties, which may be advantageous for specific applications. The advantages of rotary swaging include high production rates, increased strength and durability, precision and consistency [28]

CHAPTER 2

LITERATURE REVIEW

This literature survey aims to provide a comprehensive overview of the current state research and development in magnesium alloy materials while also addressing their advantages and limitations, ultimately shedding light on the prospects and challenges that these alloys present in the pursuit of more sustainable and efficient technologies.

Kenneth Kanayo et al. (2017) conducted a comprehensive review on Mg and its alloys with regards to its low formability due to their HCP crystal. Several research efforts have been made to enhance plastic deformability in Mg alloys through processing strategies such as alloying, traditional forming, and severe plastic deformation (SPD). Grain refinement, homogenizing of phases, reducing CRSS between slip modes, twinning suppression, and weakening and randomization of the basal texture have been explored as formability enhancing strategies. The limitations of these strategies are also discussed, along with suggestions for future areas of exploration.

Young-Gil Jung et al. (2021) investigated the effects of calcium (Ca) addition on the microstructure and mechanical properties of a Mg-6.0Zn-1.2Y-0.7Zr alloy. The addition of Ca improved the ignition resistance of the alloy and resulted in the formation of the τ -phase and Mg₂Ca. The grain size of the alloy decreased with an increase in the Ca content. The heat treatment-induced precipitation of MgZn' precipitates improved the tensile and creep properties of the alloy. The T6-treated alloy with 0.7Ca exhibited the best mechanical properties at both room temperature and 150 °C.

Sihang You et al. (2017) conducted an extensive survey on recent research and developments on wrought magnesium alloys. It specifically discusses the alloy design and the effects of different alloying elements on the microstructure and mechanical properties of these alloys. The article also mentions future research to improve the mechanical properties of wrought magnesium alloys.

Arun Bobby et al. (2013) investigated the effect of individual and combined additions of antimony (Sb) and yttrium (Y) on the microstructure and mechanical properties of AZ91

magnesium alloy. The results show that the addition of Sb and Y refines the grain size and leads to the formation of thermally stable intermetallic compounds. The combined addition of 0.6% Y and 0.5% Sb produces the best results in terms of grain refinement and mechanical properties. The ultimate tensile strength and hardness of the alloy are improved at both room temperature and elevated temperatures. The addition of Y and Sb also reduces the amount of Mg₁₇Al₁₂ phase in the alloy, resulting in improved thermal stability and grain-boundary strength.

Wang Hai-lu et al. (2011) investigate the effect of hot rolling on the microstructure, mechanical properties, and fracture behaviour of AZ40 magnesium alloy. The results show that hot rolling improves microstructure homogeneity and refines grain size through dynamic recrystallization. As a result, the mechanical properties of the as-rolled sheets are significantly improved compared to the starting as-extruded alloy.

Deepu Joy et al. (2021) in their research paper discuss the effects of zirconium (Zr) additions on the microstructure and mechanical properties of hot rolled Al-Mg alloys. The study investigates the crystalline nature, grain size, and mechanical strength of the alloys with and without zirconium additions. The addition of Zr also reduces the grain size and increases the strength of the alloys. The mechanical properties of the alloys, such as ultimate tensile strength and yield strength, are improved with the addition of Zr. However, the addition of Zr reduces the elongation of the alloy, making it less ductile. Fractography studies show that the addition of Zr leads to embrittlement and intergranular rupture. Overall, the addition of Zr improves the strength of the alloys but reduces their ductility.

Huseyin sevik et al. (2009) in their research paper discusses the effect of tin (Sn) addition on the microstructure and mechanical properties of a magnesium-based alloy (AM60). The study found that adding tin effectively decreased the size of the eutectic phase on the grain boundary and increased the hardness value of the alloy. The tensile testing results showed that the alloy with the highest tin content (4 wt% Sn) exhibited the greatest ultimate tensile strength (212 MPa). The impact strength of the alloy was also increased with a small amount of tin addition (0.5 wt% Sn), but started to decrease with further addition of tin. The addition of Sn changes the microstructure of the alloy, refining the eutectic phase on the grain boundary and decreasing the size of Mg₁₇Al₁₂ particles. The hardness of the alloy increases with increasing Sn

concentration, with the highest hardness value obtained at 2 wt% Sn. The tensile strength of the alloy also increases with increasing Sn concentration, while the elongation of the alloy decreases. The impact energy of the alloy is remarkably increased by 0.5 wt% Sn, but then decreases with increasing Sn concentration.

A.E.Davis et al. (2018) conducted a comprehensive study on reducing yield asymmetry and anisotropy in wrought magnesium alloys. The study uses several extruded and rolled magnesium alloys to evaluate the most effective strategy in developing wrought magnesium alloys in which both anisotropy and asymmetry are reduced. The study also discusses the influence of precipitation on tensile deformation and transverse-direction compressive deformation. Precipitates provide an effective strengthening mechanism that is exploited in many commercial magnesium alloys. The study uses the visco-plastic self-consistent (VPSC) model to make predictions about the relative deformation-mode activities needed to be determined, which are texture dependent. The study concludes that achieving the desired precipitate populations in a practical alloy under realistic processing conditions is difficult. Grain-size reduction is more easily achieved and is effective in reducing asymmetry, but can only combat anisotropy successfully if an alloy is not hindered by an unfavourable wrought texture.

Sung Hyuk Park et al. (2014) conducted an exceptional research and discussed the behaviour of magnesium alloys under tension and compression. The article explains that magnesium alloys have different yield strengths under tension and compression due to their texture and the polar nature of deformation twinning. The article also discusses the differences in $\{10\bar{1}2\}$ twinning behaviour under tension and compression, which results in a lower yield strength and higher strain hardening under tension than compression.

CHAPTER 3

EXPERIMENTATION

The following procedures are carried out and repeated for the preparation of three types of alloy samples viz., Mg-0.3%wtZr alloy, Mg-0.3%wtSn alloy, Mg-0.3%wtZr-0.3%wtSn alloy.

Mg-0.3%wtZr-0.3%wtSn alloy is explained elaborately as follows,

3.1. EQUIPMENT AND SETUP FOR VACUUM STIR CASTING

The essential equipment and components involved in the process are

3.1.1. FURNACE

The furnace is a crucial component in vacuum stir casting, as it's responsible for melting the metal or alloy to be cast. There are various types of furnaces used in this process, including induction furnaces, resistance furnaces, and arc furnaces. The choice of furnace depends on factors such as the type of material being cast, the desired casting temperature, and the size of the casting. In vacuum stir casting, the furnace must be capable of reaching and maintaining high temperatures to melt the metal or alloy. Induction furnaces are commonly used because they offer precise temperature control and uniform heating. These furnaces work by inducing electrical currents within the metal charge, heating it rapidly and efficiently.

3.1.2. STIRRING MECHANISM

The stirring mechanism is essential for ensuring homogeneity and uniformity in the molten metal or alloy during the casting process. This mechanism typically consists of a stirring rod or shaft that is inserted into the crucible containing the molten metal. The stirring rod is connected to a motorized drive system that rotates it at a controlled speed. The stirring action helps to disperse any alloying elements evenly throughout the molten metal, ensuring that the resulting cast product has consistent mechanical properties. It also helps to remove any gas or impurities that may be present in the molten metal, leading to a higher-quality final product.

3.1.3. CRUCIBLE

The crucible is a container used to hold the metal or alloy during the melting process. It must be made of a material that can withstand high temperatures without melting or deforming, such as graphite, ceramic, or refractory metals. Crucibles come in various sizes and shapes, depending on the specific requirements of the casting process. They are designed to withstand the harsh conditions inside the furnace and provide a stable environment for melting and holding the molten metal. It is generally made of Alumina and holds the magnesium matrix and reinforcement materials during the stirring process.

3.1.4. STIRRING TOOLS

Stirring tools refer to the implements used to manipulate the stirring mechanism and control the movement of the molten metal within the crucible. These tools can vary depending on the design of the stirring mechanism and the specific requirements of the casting process. Common stirring tools include stirring rods, paddles, and blades, which are attached to the stirring mechanism and used to agitate the molten metal. The design and material of the stirring tools are critical to ensure efficient mixing and dispersion of alloying elements throughout the molten metal.

3.1.5. COOLING SETUP

The cooling setup is essential for controlling the solidification process of the cast metal and preventing defects such as shrinkage, porosity, and cracking. This setup typically consists of a cooling chamber or system that is used to rapidly cool the cast metal after it has been poured into the mould. There are various cooling methods used in vacuum stir casting, including water quenching, air cooling, and controlled cooling using specialized cooling chambers. The choice of cooling method depends on factors such as the type of metal or alloy being cast, the desired cooling rate, and the size and complexity of the casting.

3.1.6. GAS SUPPLY

The gas supply is used to create a vacuum environment inside the casting chamber, which is essential for removing gases and impurities from the molten metal and preventing oxidation during the casting process. Common gases used in vacuum casting include argon, nitrogen, and helium. The gas supply system typically consists of gas cylinders, regulators, valves, and vacuum pumps, which are used to create and maintain the desired vacuum pressure inside the casting chamber. The gas is introduced into the chamber through a series of nozzles or ports, and the vacuum pump is used to remove excess gas and maintain the desired pressure.

3.1.7. VACUUM CHAMBER

The vacuum chamber is the heart of the vacuum stir casting setup, where the entire casting process takes place. It is a sealed enclosure that is capable of creating and maintaining a vacuum environment, typically with pressures ranging from a few millibars to several hundred millibars. The vacuum chamber is constructed from materials that can withstand high temperatures and vacuum conditions without deforming or leaking, such as stainless steel or high-strength alloys. It is equipped with various ports, valves, and fittings for connecting the gas supply, vacuum pump, and other auxiliary equipment. Inside the vacuum chamber, the crucible containing the molten metal is placed on a platform or pedestal, and the stirring mechanism is inserted into the crucible. The chamber is then sealed, and the vacuum pump is activated to create the desired vacuum pressure. Once the vacuum is established, the furnace is heated to melt the metal or alloy, and the stirring mechanism is activated to agitate the molten metal and ensure uniform mixing and dispersion of alloying elements.



Fig 3.1: Experimental set-up of vacuum stir casting equipment

3.2. MATERIAL SELECTION

Magnesium is the primary material with Zirconium (0.3%) and Tin (0.3%) are added as reinforcing materials. Zirconium is chosen for its ability to enhance the mechanical properties such as strength and stiffness and tin is added to improve the castability..

3.3. STIR CASTING PROCEDURE

The selected magnesium alloy is placed in the crucible and the furnace is used to heat the matrix material to its melting point under vacuum condition. With magnesium in molten state, Zirconium and Tin particles are added. Stirring process is carried out to ensure even distribution of reinforcement materials within the molten magnesium matrix, to break up any agglomerate formation and promote homogeneity of the mixture by continuous agitation. Degassing is carried out simultaneously to remove dissolved gases and impurities from the molten magnesium and enhancing the quality through the use of vacuum chamber, inert gas bubbling or the addition of degassing agents. The cast alloy was homogenized at 723 K for 4 hours. Once the stirring process is complete and the desired dispersion is achieved, the composite material is quenched to cool and solidify. It is then trimmed and machined for the hot rolling process.

3.4. HOT ROLLING OF Mg-0.3%wtZr-0.3%wtSn alloy

3.4.1. EQUIPMENT AND SETUP FOR HOT ROLLING

3.4.1.1. ROLLING MILL

The heart of the hot rolling process is the rolling mill. A rolling mill is a complex machine that consists of set of rolls (usually two or more) mounted on a sturdy frame. These rolls exert compressive forces on the metal or alloy being processed, reducing its thickness and changing its shape. The rolls are typically made of high-strength steel and have various surface textures to impart specific finishes or textures to the rolled material.

3.4.1.2. HEATING FURNACE

A heating furnace is used to bring the ingot or billet to the required rolling temperature. The temperature is carefully controlled to achieve the desired material properties and ensure uniform deformation during rolling.

3.4.1.3. ROLL GAP ADJUSTMENT

Roll gap adjustment mechanism allow for control over the thickness reduction and shape changes during the rolling process. Precise adjustments are made to achieve the desired final dimensions of the rolled material.

3.4.1.4. COOLING SYSTEM

After the material passes through the rolls, it may be subjected to cooling to control its temperature and microstructure. Water-based cooling systems, like spray systems or quench tanks are often employed for this purpose.

3.4.1.5. CONVEYORS

Material handling and transportation equipment such as conveyors or manipulators are used to move the ingot or slab from the heating furnace to the rolling mill and then to the cooling system.



Fig 3.2: Experimental set-up of Hot Rolling Equipment

3.4.2. HOT ROLLING PROCEDURE

The Mg-Zr-Sn alloy ingot is loaded into a heating furnace. A heating temperature of 350°C to 450 °C is applied in a carefully controlled manner as magnesium has relatively lower melting point. Once the Mg-Zr-Sn alloy reaches the desired

rolling temperature, it is transported to the rolling mill. The rolls of the mill are pre-adjusted to the desired roll gap, which determines the final thickness and shape of the rolled material. The Mg-Zr-Sn alloy enters the rolling mill and passes through the rolls. The compressive forces applied by the rolls reduce the thickness of the ingot and shape it according to the roll profiles. The ingot is continuously passed through the rolls in multiple cycles until the desired dimensions and shape are achieved. During the rolling process, adjustments to the roll gap are made to achieve the target thickness. The degree of thickness reduction is controlled by the roll gap, number of passes and rolling speed. In addition to thickness reduction, hot rolling can impart specific changes to the material. This is achieved by using rolls with varying profiles and adjusting the roll gap accordingly. Shape changes include production of flat sheets, plates or structural sections.

3.5. CUTTING AND GRINDING OF STIR CAST Mg-0.3%wtZr-0.3%wtSn alloy

3.5.1. CUTTING

The sample is securely clamped to prevent movement during the cutting process. The diamond wheel saw is gradually lowered onto the sample's surface and the sample cutting is initiated. Lubrication with cutting oil is critical to reduce friction, heat and wear on the cutting tool. Once the cut is completed, the equipment is safely shut down, the clamps or vices are removed and the cut sample is carefully extracted.

3.5.2. GRINDING

The process begins with the preparation of grinding equipment where abrasive discs or wheels are attached to a grinder, selection of grinding parameters such as wheel speed, pressure and direction. Even pressure is applied and consistently maintained to ensure uniform material removal and avoiding overheating.

Grinding wheel type: CBN (Cubic Boron Nitride)

Wheel speed: 6000 RPM

Depth of Cut: 30 μm

Feed rate: 0.4 mm/rev

Coolant/Lubricant: Water-soluble oil-based coolant

Wheel grit size: Coarse grit -60 to 120 mesh

Fine grit-120 to 320 mesh

Grinding pressure: 40 psi

After reaching the desired dimensions and surface finish, a final inspection is conducted to verify that the sample meets the specified requirements, and any remaining burrs or sharp edges are removed to ensure the sample's safety and readiness for subsequent material characterization.

3.6. MOUNTING

Mounting process involves embedding the sample in epoxy resin (mounting material) to provide stability, support, and the protection for subsequent process. The resin is poured in to the mould covering the sample while taking care to avoid entrapping air bubbles. In order to remove the air bubbles the mould is generally placed in a vacuum chamber or subjected to vibration. The mounted sample is allowed to cure typically through a thermal process, hardening the resin to securely hold the sample in place. After curing, the mounted sample is carefully removed from the mould and any excess resin is trimmed and polished creating a flat and smooth surface for subsequent processing.

3.7. POLISHING

Polishing Mg-Zr-Sn alloy involves a sequence of steps using a progressively finer abrasive to achieve the desired surface finish.

3.7.1. Coarse Grinding(Grade #120 to #320)

- 3.7.1.1. The initial step involves embedding the Mg-0.3Zr-0.3Sn alloy sample in a mounting resin. This ensures stability during the polishing process and provides a flat, uniform surface for subsequent steps.
- 3.7.1.2. Coarse grinding is the first abrasive step, using a metal-bonded diamond abrasive disk with a grit size of #120. This step removes excess material

rapidly and levels the sample surface. Water is typically used as a coolant and lubricant during grinding to prevent overheating.

3.7.1.3. The sample is then subjected to medium grinding using a diamond abrasive disk with a finer grit size of #240. This further refines the surface and prepares it for the subsequent polishing steps.

3.7.1.4. Fine grinding is performed using a diamond abrasive disk with a grit size of #320. This step continues the material removal process while achieving a smoother surface finish. The sample is regularly rotated and repositioned to ensure uniform grinding.

3.7.2. Fine Grinding(#400 to #600)

3.7.2.1. The sample undergoes fine grinding using a diamond abrasive disk with a grit size of #400. This step aims to remove the scratches and deformation marks left by the coarse grinding process while preparing the surface for the subsequent finer abrasive steps.

3.7.2.2. Extra fine grinding is carried out using a diamond abrasive disk with a grit size of #600. This step further refines the surface, minimizing any remaining scratches and preparing the sample for the polishing stages. Careful attention is given to the pressure applied to avoid introducing artefacts.

3.7.3. Polishing (Grade #800 to #1200)

3.7.3.1. The polishing process begins with a diamond suspension of grit size #800. This step involves using a rotating polishing cloth with the abrasive suspension to create a mirror-like finish on the sample surface. The pressure and polishing time are controlled to achieve optimal results.

3.7.3.2. Further refinement is achieved through polishing with a finer diamond suspension of grit size #1200. This step aims to eliminate any remaining scratches and enhance the surface smoothness, preparing the sample for the final polishing steps.

3.7.4. Final Polishing(Grade #2000 to #4000)

3.7.4.1. Final polishing commences with a diamond suspension of grit size #2000. This step focuses on achieving a superior surface finish, removing any fine scratches left from the previous polishing stages.

3.7.4.2. The last polishing step involves using a diamond suspension of grit size #4000. This fine polishing step ensures that the Mg-0.3%wtZr-0.3%wtSn alloy sample's surface is free from any visible scratches or artefacts, resulting in a polished surface suitable for detailed microstructural analysis.

3.7.5. Cleaning and inspection

After polishing, it is essential to clean the alloy sample thoroughly to remove any abrasive residues. The polished surface is inspected for any remaining imperfections, scratches, or defects. If necessary, repeat the final polishing step.

The same procedures are followed for the preparation of Mg-0.3%wtZr alloy and Mg-0.3%wtSn alloy.

CHAPTER 4

MATERIAL CHARACTERISATION TECHNIQUES

4.1. ULTIMATE TENSILE TEST

The ultimate tensile test machine, also known as a universal testing machine (UTM) or a tensile testing machine, is a vital instrument used to determine the mechanical properties of materials under tension. It applies controlled tensile forces to a specimen until it fractures, providing valuable data for material characterization and quality assurance in various applications.

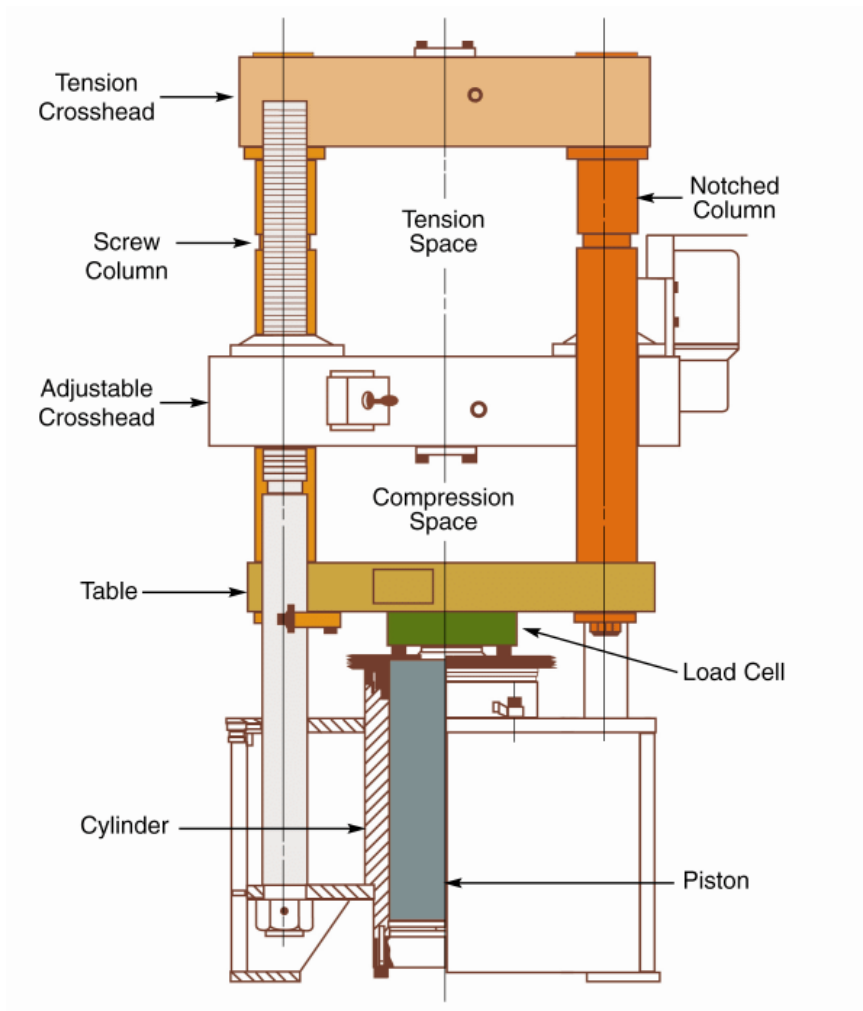


Fig 4.1: Experimental set-up of Ultimate Tensile Test [41]

The Ultimate Tensile Test machine consists of several essential components which includes

a. Load Frame

The load frame is the main structural component of the tensile test machine, providing support and rigidity during testing. It houses the moving crosshead, grips, and other accessories necessary for specimen fixation and loading.

b. Crosshead

The crosshead is a movable part of the load frame that applies tensile or compressive forces to the specimen. It is driven by a motorized drive system and guided along precision rails to ensure accurate alignment and loading.

c. Grips

Grips are specialized fixtures used to securely hold the specimen during testing. They come in various designs depending on the type and geometry of the specimen. Common grip types include wedge grips, pneumatic grips, hydraulic grips, and serrated jaws.

d. Load cell

The load cell is a transducer that converts mechanical force into electrical signals. It measures the applied load exerted on the specimen during testing with high accuracy and resolution. Load cells are available in different capacities to accommodate a wide range of load requirements.

e. Displacement sensor

The displacement sensor, also known as an extensometer, measures the deformation or elongation of the specimen during testing. It provides precise displacement readings, allowing for accurate determination of strain and elongation at various stages of the test.

f. Control system

The control system comprises electronic hardware and software responsible for regulating the testing parameters, controlling the test procedure, and acquiring data. It allows users to set test parameters such as loading rate, test speed, and data acquisition frequency.

g. Data Acquisition System(DAQ)

The data acquisition system collects, processes, and records data generated during the tensile test. It interfaces with the load cell, displacement sensor, and

other sensors to capture load, displacement, and other relevant parameters in real-time. [40]

The operation of the ultimate tensile test includes the following

1. The sample is machined to a flat dog-bone shape with a gauge length of 50.8 mm and mounted into the testing machine's grips ensuring proper alignment and secure fixation.
2. The sample is securely mounted between the grips of the tensile test machine. The grips may be adjusted to accommodate different specimen geometries and sizes. Proper alignment and centering of the specimen ensure accurate loading and prevent premature failure.
3. Once the sample is installed, the following test parameters are set
Gauge length- 13 mm
Diameter-4 mm
Thickness-2.7 mm
Crosshead speed-2mm/min
Room temperature-25°C
Load- 2KN
Sampling rate- 10 Hz (10 data points per second)
4. A small preload is applied to the specimen to ensure proper contact between the grips and the specimen. The preload value is typically a small percentage of the expected ultimate load and helps eliminate any slack or initial deformation in the setup.
5. With the sample under preload, the tensile test begins by applying an axial load to the specimen at a constant rate of displacement or strain. The load is continuously increased until the specimen fractures or reaches its ultimate tensile strength. Throughout the test, load and displacement data are recorded by the data acquisition system.
6. After testing, the acquired data, including load-displacement curves, stress-strain curves, and mechanical properties, are analysed using specialized software or data analysis tools. The results are interpreted to evaluate the material's mechanical behaviour, including its strength, ductility, toughness, and stiffness.

7. The test results, along with relevant information such as specimen details, testing conditions, and testing standards used, are documented in a comprehensive test report. This report serves as a formal record of the test and is often required for quality control, material certification, and research purposes.
8. The same procedures are followed in compression to determine the same parameters under compressive loading condition.

4.2. SEM- EBSD OBSERVATIONS

Scanning Electron Microscopy is a powerful instrument used for material characterisation to visualise the material at extremely high resolution, magnification and depth of field. It uses a focused beam of electrons instead of light to image the specimen.

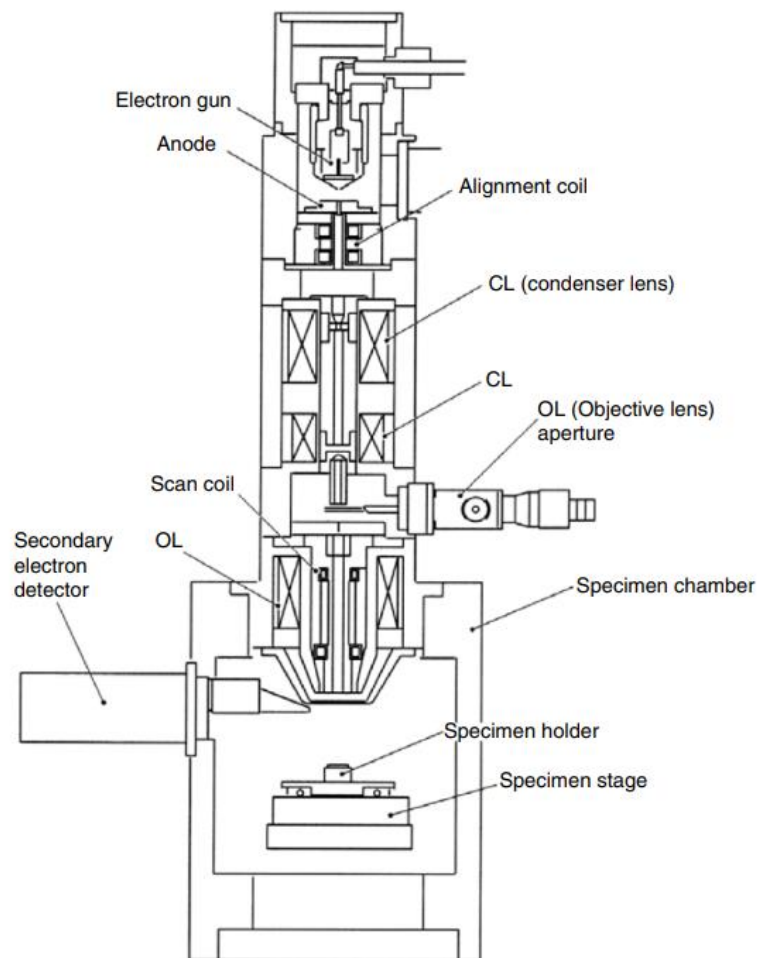


Fig 4.2: Schematic representation of Scanning Electron Microscope [34]

When the electron beam interacts with the specimen's surface, various signals are generated such as Secondary Electrons (SEs), Back Scattered Electrons (BSEs) and characteristic X-rays.

These signals provide information about the specimen's surface topography, composition and crystallographic structure.

The major components of the SEM are vacuum system, electron beam generation system, electron beam manipulation system, beam specimen interaction system, detection system, signal processing system and display and record system.

1. Vacuum System

The primary function of the vacuum system is to create and maintain a high-vacuum environment inside the SEM chamber. High vacuum is necessary to prevent air molecules from scattering the electron beam, which could degrade the image quality and resolution. By evacuating air and other gases from the chamber, the vacuum system helps preserve the integrity of the electron beam, minimize sample contamination, and facilitate accurate sample analysis. It comprises various sub-components like vacuum pumps, gauges, valves and the vacuum chamber working together to ensure the instrument's proper operation and the generation of high-quality image and data.

a. Vacuum pumps

Vacuum pumps are responsible for removing air and other gases from the chamber, creating necessary vacuum environment. The types of vacuum pumps used are

1. Turbo-molecular pumps:

Turbo-molecular pumps are one of the primary pumps used in SEM vacuum systems. They operate based on the principle of momentum transfer. This pump consists of a series of rapidly spinning rotor blades that impart momentum to gas molecules, causing them to move towards the exhaust port. Turbo-molecular pumps can achieve high vacuum levels and are highly efficient at pumping gases in the low-to-medium pressure range.

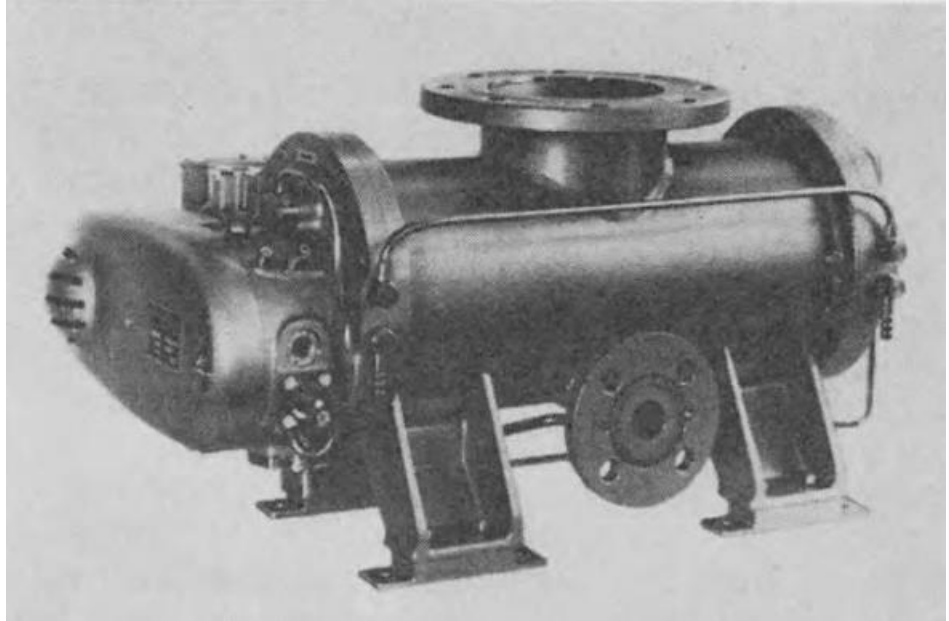


Fig 4.3: Image describing pump set-up in vacuum system [43]

2. Ion pumps:

Ion pumps operate by ionizing gas molecules and then capturing the ions on a surface within the pump, effectively removing them from the vacuum chamber. Ion pumps are capable of achieving ultra-high vacuum levels and are particularly effective at removing reactive gases and maintaining a clean vacuum environment.

3. Rotary vane pumps:

Rotary pumps are mechanical pumps that utilize rotating vanes to compress gas and create vacuum. These pumps are commonly used as backing pumps to support turbo-molecular or ion pumps by providing pre-vacuum or medium vacuum levels. Rotary vane pumps are relatively simple, reliable, and cost-effective and making them a popular choice for SEM vacuum systems.

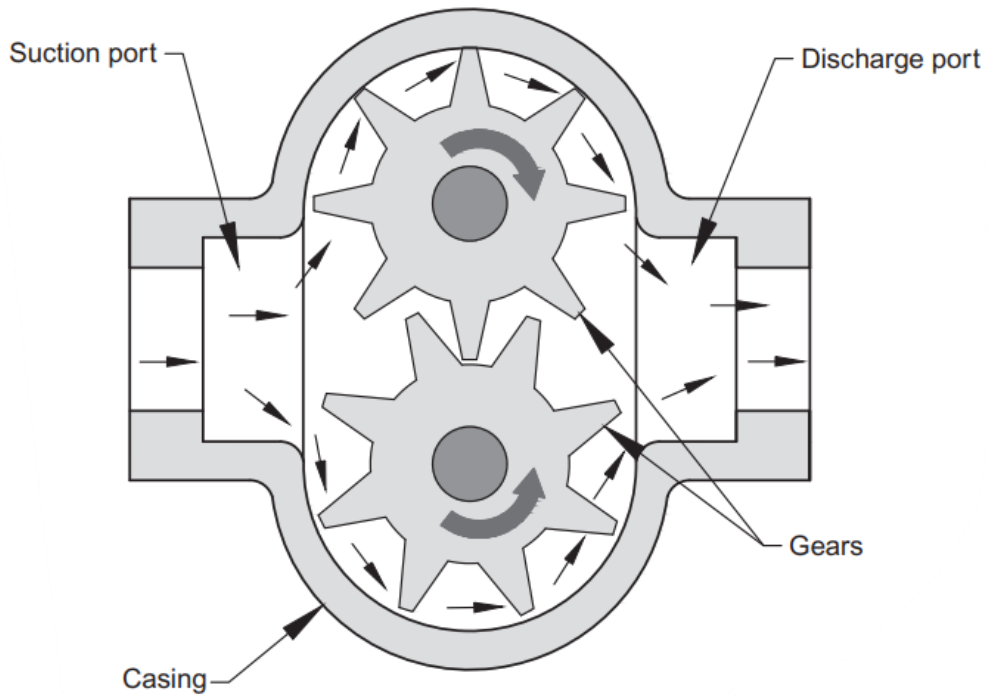


Fig 4.4: Sketch representing direction of air flow across the pump [43]

4. Scroll pumps:

Scroll pumps are oil-free mechanical pumps that use interlocking spiral-shaped scrolls to compress gas and create vacuum. They are known for quiet operation, low vibration and minimal maintenance requirements. Scroll pumps are often used in combination with other pumps such as turbo-molecular or ion pumps to providing roughing or medium vacuum levels in SEM systems.

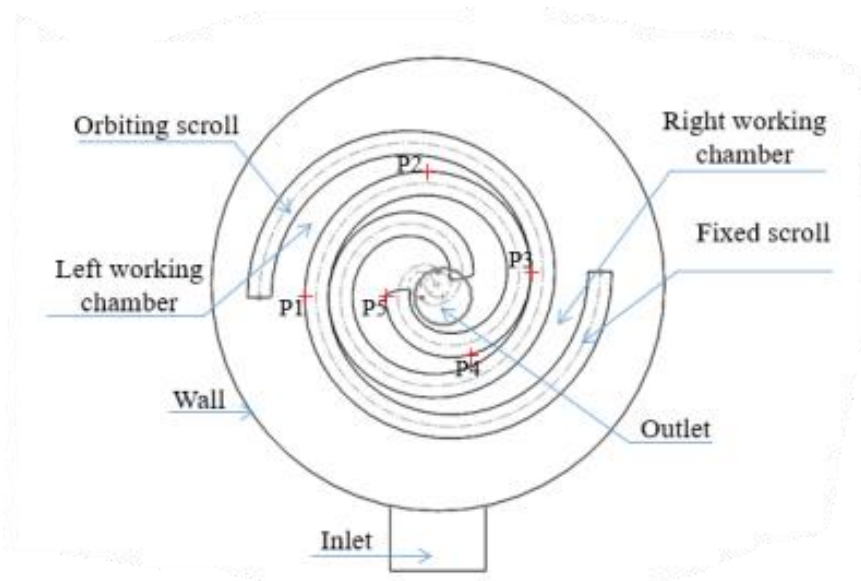


Fig 4.5: Diagram representing components of scroll pumps [43]

b. Vacuum gauges

Vacuum gauges are essential instruments which provide accurate measurements of the pressure inside the specimen chamber, allowing operators to monitor and control the vacuum level for optimal SEM performance. Common types of vacuum gauges used are

1. Penning gauges:

Penning gauges operate based on the ionization of gas molecules in a low-pressure environment. They consist of an anode and a cathode separated by a small gap filled with a gas, typically a noble gas such as argon. When a voltage is applied between the anode and cathode, gas molecules in the gap are ionized, and the resulting ions create a current flow between the electrodes. The magnitude of this current is proportional to the pressure inside the gauge, allowing for pressure measurement. Penning gauges are known for their wide pressure measurement range, from high vacuum to medium vacuum levels.

2. Pirani gauges:

Pirani gauges operate based on the thermal conductivity of gas molecules. They consist of a heated wire or filament placed in the vacuum chamber. As gas molecules collide with the heated filament, they transfer heat away from the filament, causing its temperature to decrease. The filament's temperature is monitored, and the pressure inside the chamber is inferred from the rate of temperature decrease. Pirani gauges are commonly used for measuring pressures in the medium-to-high vacuum range.

3. Cold cathode Ionization gauges:

Cold cathode ionization gauges are similar to Penning gauges but use a cold cathode instead of a hot cathode. They rely on the ionization of gas molecules by electrons emitted from the cold cathode. The resulting ions create a current flow between the cathode and anode, which is proportional to the pressure inside the gauge. Cold cathode ionization gauges are capable of measuring pressures in the high vacuum range and are often used as backup gauges in SEM systems.

4. Hot filament ionization gauges:

Hot filament ionization gauges utilize a heated filament to emit electrons, which ionize gas molecules in the vacuum chamber. The resulting ions create a current flow between the filament and an electrode, allowing for pressure measurement. Hot filament ionization gauges are sensitive to changes in pressure and are commonly used for measuring pressures in the high vacuum range.

c. Vacuum valves

Vacuum valves serves various purpose including controlling the flow of gases, isolating different parts of the vacuum system and facilitating specimen exchange. Different types of vacuum valves employed are

1. Gate valves:

Gate valves are typically actuated using pneumatic or motorized mechanisms for remote operation. They are often used to isolate the specimen chamber during pump-down or venting procedures and to separate the specimen chamber from other components of the SEM vacuum system.

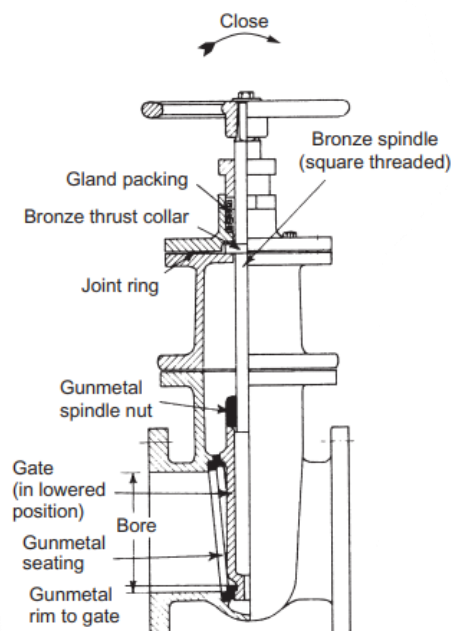


Fig 4.6: Schematic sketch of gate valve [43]

2. Butterfly valves:

Butterfly valves consist of a disk-shaped valve element mounted on a central axis. When the valve is open, the disk rotates to allow gas

to pass through, and when closed, it seals against the valve seat to prevent gas flow. Butterfly valves are commonly used in roughing lines and for venting large volumes of gas from the vacuum system quickly.

3. Needle valves:

Needle valves are precision valves used for fine control of gas flow rates in SEM vacuum systems. They consist of a tapered needle that fits into a valve seat. By adjusting the position of the needle relative to the seat, the flow rate through the valve can be precisely controlled. Needle valves are often used in conjunction with pressure controllers or mass flow controllers to regulate gas flow during sample preparation or gas injection processes.

4. Angle valves:

Angle valves are compact valves used in SEM vacuum systems for connecting vacuum components at non-linear angles. They feature a 90-degree bend in their design, allowing them to be mounted in tight spaces or at right angles to the vacuum line. Angle valves are commonly used for connecting vacuum chambers, pumps, and other components in SEM systems while maintaining a low profile.

5. Isolation valves:

Isolation valves are used to isolate specific components or sections of the vacuum system for maintenance, repair, or troubleshooting purposes. These valves allow operators to close off a particular section of the vacuum system without affecting the rest of the system's operation. Isolation valves are typically installed at strategic points in the vacuum system, such as between pump stages or before critical components like the electron gun or specimen chamber.

6. Venting valves:

Venting valves are used to introduce gas into the vacuum system to backfill the chamber or to introduce specific gases for sample preparation or analysis. These valves allow controlled venting of the vacuum system without compromising its overall integrity. Venting valves are often equipped with pressure regulators or flow

controllers to ensure precise control over the gas flow rate and pressure.

d. Vacuum chamber:

The heart of the vacuum system, the vacuum chamber houses the electron column and the specimen stage. It is typically made of high-quality stainless steel or other materials capable of withstanding high vacuum pressures. The chamber is sealed to prevent air from entering and maintain the desired vacuum level. The functions of vacuum chamber includes

1. Maintaining low pressure:

The primary function of the vacuum chamber is to maintain a vacuum environment with pressures typically ranging from high vacuum (10^{-3} to 10^{-7} Torr) to ultra-high vacuum (below 10^{-7} Torr). This low-pressure environment is necessary to ensure that the electrons emitted by the electron source travel without significant collisions with gas molecules, allowing for high-resolution imaging.

2. Isolation of specimen:

The vacuum chamber isolates the specimen being imaged from the surrounding atmosphere. This isolation prevents contamination of the specimen by atmospheric gases or particulates, ensuring that the sample remains clean and undisturbed during imaging.

3. Electron beam path:

The vacuum chamber provides a path for the electron beam emitted by the electron gun to travel from the electron source to the specimen. The low-pressure environment inside the chamber minimizes electron scattering and absorption by gas molecules, allowing the beam to reach the specimen with minimal interference.

4. Specimen manipulation:

The vacuum chamber includes mechanisms for manipulating the specimen, such as stages for positioning and tilting the sample. These mechanisms allow precise control over the orientation and position of the specimen relative to the electron beam for imaging and analysis.

5. Detectors and signal collection:

The vacuum chamber house detectors and other components used for collecting signals generated by interactions between the electron beam

and the specimen. These detectors need to be situated within the vacuum environment to prevent signal loss due to gas molecules scattering or absorbing electrons.

2. Electron Beam generation system

The electron beam in an SEM is the primary tool used for imaging and analysis of specimens at high magnifications and resolutions. The generation of electron beam in an SEM involves several types of emission

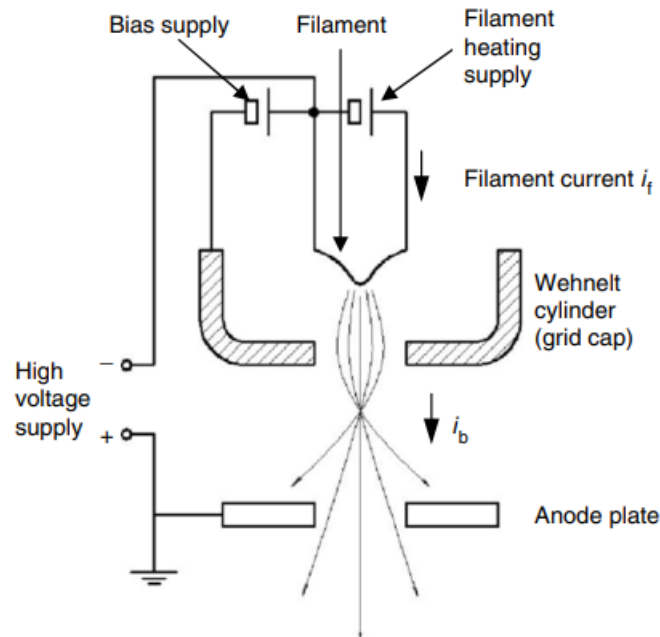
2.1. Thermionic emission

Thermionic emission, also known as thermal electron emission, is one of the primary methods for generating electron beams in SEMs. It occurs when electrons are emitted from a heated filament, typically made of tungsten, due to thermal energy. The high temperature of the filament causes electrons to overcome the work function barrier and escape into the vacuum chamber. In SEMs, a heated tungsten filament serves as the electron source. The filament is placed within an electron gun assembly, where it is heated to temperatures typically ranging from 2000°C to 3000°C. The emitted electrons are then focused and accelerated towards the sample surface.

2.2. Field emission

Field emission, also referred to as cold emission or field electron emission, occurs when electrons tunnel through a potential barrier under the influence of a strong electric field. In SEMs, field emission can be achieved using a sharp tip or edge geometry, which concentrates the electric field and facilitates electron emission. Field emission electron sources are utilized in high-resolution SEMs to achieve superior spatial resolution and imaging capabilities. Carbon nanotubes or other Nano scale structures are often employed as field emitters due to their sharp tips and high electric field enhancement factors.

The electron beam is generated using an electron gun assembly which typically consists of a filament, wehnelt cylinder, anode, and various lenses and detectors.



4.7: Diagram describing the field emission [34]

a. Filament or cathode

In SEMs utilizing a tungsten filament, the filament serves as the cathode. It is typically heated to temperatures ranging from 1,500 to 2,500 degrees Celsius. At such high temperatures, thermionic emission occurs, and electrons are liberated from the surface of the filament. Once emitted from the cathode, the electrons are accelerated towards the anode (or electron optical column) through the application of a high voltage. This acceleration is achieved using an electric field generated between the cathode and anode.

b. Wehnelt cylinder or anode

The anode, also known as the Wehnelt cylinder, is a positively charged electrode located near the electron source. Its primary function is to control the electron beam's focusing and intensity. It achieves this by acting as an electrostatic lens, which helps converge and focus the electrons into a narrow beam.

c. Aperture

An aperture may be included in the electron gun assembly to control the size and shape of the electron beam. It acts as a physical barrier, limiting

the spread of electrons and ensuring that only a well-defined portion of the beam reaches the specimen

d. Electrostatic lenses

Electrostatic lenses are crucial components within the electron gun assembly. They manipulate the trajectory of the electron beam, controlling its direction and focusing it onto the specimen. These lenses typically consist of a series of positively and negatively charged electrodes arranged in a specific configuration to shape and focus the electron beam.

e. Condenser lens

The condenser lens, situated near the electron source, further focuses the electron beam before it enters the electron optical column. Its role is to enhance the beam's coherence and intensity, ensuring optimal imaging performance.

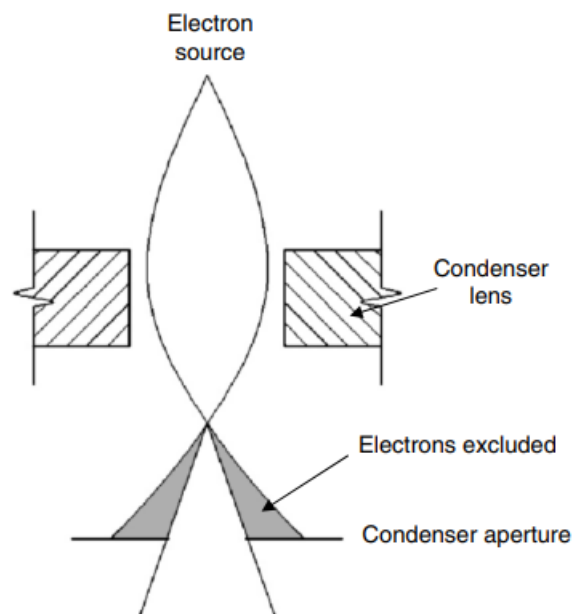


Fig 4.8: Diagram describing condenser lens [34]

f. Electron optical column

The electron optical column encompasses the entire pathway through which the electron beam travels from the electron source to the specimen. It consists of various electromagnetic and electrostatic lenses, deflectors,

and apertures arranged in a precise configuration to manipulate and control the electron beam's properties.

g. Beam scanning system

Within the electron optical column, a beam scanning system is employed to raster the electron beam across the specimen's surface. This scanning mechanism typically consists of electromagnetic coils or deflectors that rapidly deflect the electron beam in both the horizontal and vertical directions, allowing it to cover the entire specimen area systematically.

h. Beam alignment and stigmation

Proper alignment and stigmation of the electron beam are essential for achieving high-resolution imaging in an SEM. Alignment ensures that the electron beam is centred and focused on the specimen, while stigmation corrects any astigmatism in the beam's shape, improving image clarity and resolution.

i. Electron detectors

At the end of the electron optical column, specialized detectors capture signals generated by interactions between the electron beam and the specimen. These detectors may include secondary electron detectors, backscattered electron detectors, and energy-dispersive X-ray spectroscopy (EDS) detectors, each providing unique information about the specimen's surface composition, topography, and elemental composition.

3. Electron beam detection system

The electron beam detection system plays a crucial role in capturing and analysing signals emitted from the sample surface when it interacts with the electron beam. This system comprises various detectors to detect different types of signals including secondary electrons, backscattered electrons and characteristic X-rays.

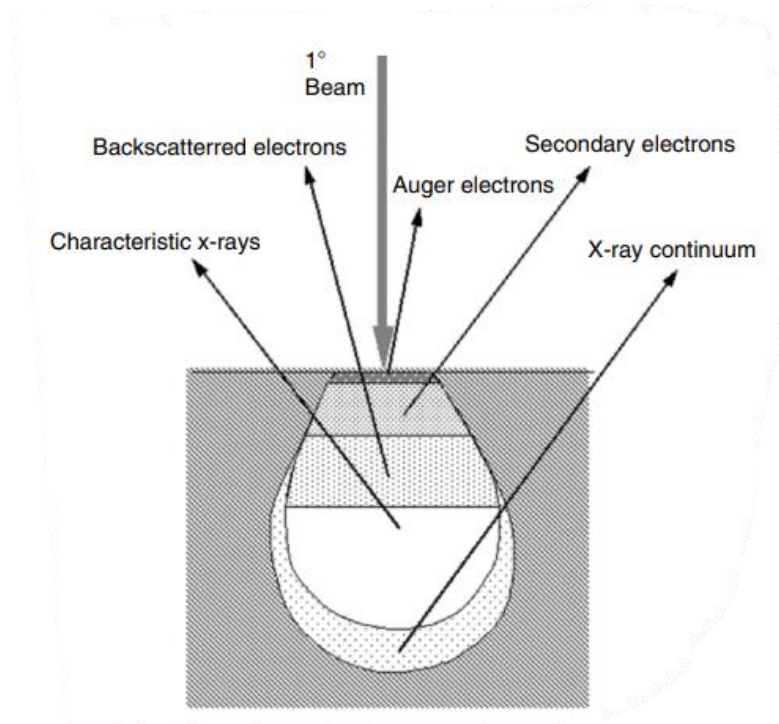


Fig 4.9: Depiction of various electron scattering [34]

3.1. Secondary Electron(SE) detection:

When the primary electron beam interacts with the atoms in the specimen's surface, it can dislodge secondary electrons from the specimen. These secondary electrons carry valuable information about the surface topography and composition. Secondary electrons are typically low in energy and emitted from the top few nanometres of the specimen's surface. To detect them, SEMs employ secondary electron detectors positioned above the specimen. These detectors typically consist of scintillators or semiconductor materials capable of converting incoming secondary electrons into visible light or electrical signals. Secondary electron detection can be performed in various modes, including secondary electron imaging (SEI), where the detector collects secondary electrons to generate high-resolution images revealing surface topography.

3.2. Backscattered Electron (BSE) detection:

When the primary electron beam interacts with the atoms in the specimen's surface, some electrons are scattered backward (backscattered electrons). The intensity of backscattered electrons depends on the atomic number and density of the specimen's constituents, providing valuable compositional

contrast. Backscattered electron detectors are positioned above the specimen and are designed to collect electrons scattered at large angles (typically greater than 90 degrees). These detectors can consist of semiconductor materials or scintillators capable of converting backscattered electrons into visible light or electrical signals. Backscattered electron detection is commonly used for compositional contrast imaging, where differences in atomic number or density within the specimen are highlighted. It can also provide topographical information when combined with secondary electron imaging.

3.3. Energy-Dispersive X-ray spectroscopy (EDS) detection:

When the primary electron beam interacts with the atoms in the specimen's surface, it can excite the atoms, causing them to emit characteristic X-rays. Each element emits X-rays at specific energies, allowing for elemental analysis of the specimen's composition. EDS detectors are positioned below the specimen to capture characteristic X-rays emitted during electron beam interaction. These detectors typically consist of semiconductor materials such as silicon drift detectors (SDDs) or silicon drift chambers (SDCs), which can efficiently capture and quantify X-ray signals. EDS analysis provides qualitative and quantitative elemental analysis of the specimen. By measuring the energies and intensities of emitted X-rays, EDS detectors can identify the elements present in the specimen and determine their concentrations.

4. Signal processing system

The signal processing system is responsible for converting raw signals detected by various detectors into interpretable images and analytical data. This system comprises a series of electronic circuits, processors, software algorithms, and user interfaces designed to amplify, filter, digitize, and analyse signals generated during electron beam-sample interactions. The aspects of signal processing system are

4.1. Signal Amplification

The signals detected by SEM detectors are often weak and require amplification to be accurately processed and analysed. Signal amplification is typically achieved using preamplifiers or signal

conditioning circuits integrated into the detectors or dedicated amplifier modules. These circuits boost the detected signals while minimizing noise and distortion. Users can adjust amplification parameters such as gain and offset to optimize signal-to-noise ratios and dynamic range according to the specific requirements of the experiment or analysis.

4.2. Filtering and Noise Reduction

SEM signals may be contaminated by various sources of noise, including thermal noise, electronic noise, and environmental interference. Filtering and noise reduction techniques are employed to enhance signal clarity and quality. Analog and digital filters are utilized to suppress noise and unwanted frequencies while preserving signal integrity. Low-pass, high-pass, band-pass, and notch filters are commonly employed to target specific noise sources and frequencies. Techniques such as averaging, median filtering, and adaptive filtering may be implemented to further reduce noise and improve signal-to-noise ratios.

4.3. Analog-to-Digital Conversion(ADC)

To facilitate digital processing and analysis, analog signals are converted into digital format through ADC converters. ADC converters sample the analog signal at regular intervals and quantize the sampled values into digital data. The resolution and sampling rate of the ADC determine the accuracy and fidelity of the digitized signal. The number of bits used for quantization determines the resolution of the digitized signal. Higher bit depths result in finer resolution but require increased computational resources. The sampling rate defines the frequency at which analog signals are sampled and converted into digital data. It must be sufficiently high to accurately capture signal dynamics and avoid aliasing.

4.4. Image Formation and Reconstruction

Digitized signals from SEM detectors are processed to generate images that visually represent the specimen's surface characteristics. Image formation involves reconstructing images pixel by pixel from the digitized signals using software algorithms. Various techniques such as pixel intensity mapping, interpolation, and edge detection may be employed to enhance image quality and detail. SEM software typically provides a range

of image processing tools for adjusting contrast, brightness, sharpness, and colour balance to optimize image visualization and analysis.

4.5. Data Analysis and Visualisation

In addition to image formation, the signal processing system enables quantitative analysis and visualization of SEM data. Software algorithms and tools are used to extract quantitative information from SEM signals, such as surface roughness, particle size distribution, elemental composition, and crystallographic orientation. Analytical results are presented through various data visualization techniques, including histograms, scatter plots, contour plots, and surface renderings, to facilitate interpretation and comparison.

4.6. Integration with control system

The signal processing system is integrated with the SEM's control system, allowing seamless coordination of data acquisition, processing, and instrument operation. Communication protocols and interfaces enable interaction between the signal processing system, detectors, imaging software, and user interfaces. Real-time feedback mechanisms ensure synchronization and optimization of data acquisition parameters.

4.7. User Interface and Interaction

The signal processing system is accessed and controlled through user-friendly interfaces, allowing researchers to configure experiments, adjust imaging parameters, and analyse data efficiently. Graphical user interfaces (GUIs) and software platforms provide intuitive controls for SEM operation, image acquisition, data analysis, and reporting. Customizable workflows and automation features streamline repetitive tasks and workflows.

5. Display and Record system

The display and record system is responsible for visualizing, capturing, and storing images and data generated during SEM operation. This system comprises various elements, including display monitors, image capture devices, data storage media, and associated software, designed to facilitate real-time observation, analysis, documentation, and archiving of SEM imaging and analytical results. The aspects of display and record system are

5.1. Display Monitors

Display monitors serve as the primary interface for visualizing SEM images and data in real-time. High-resolution LCD or LED monitors are commonly used in SEM systems to provide clear and detailed image reproduction. Multiple monitors may be employed to accommodate different viewing angles and tasks, such as specimen observation, image analysis, and data processing. Display monitors may feature adjustable brightness, contrast, and colour balance settings to optimize image visualization. Larger screen sizes and high pixel densities enhance the clarity and detail of SEM images.

5.2. Image capture devices

Image capture devices are used to record SEM images and data for further analysis, documentation, and sharing. Digital cameras or charge-coupled device (CCD) cameras are commonly employed as image capture devices in SEM systems. These cameras can be integrated into the SEM instrument or connected externally via dedicated interfaces. Image capture devices vary in resolution, sensitivity, and dynamic range, depending on the specific imaging requirements of the SEM application. High-resolution cameras with low noise and high sensitivity are preferred for capturing fine details and low-intensity signals.

5.3. Data Storage Media

Data storage media are used to store captured SEM images, spectra, and analytical results for archival and retrieval purposes. Hard disk drives (HDDs), solid-state drives (SSDs), and network-attached storage (NAS) systems are commonly used as data storage media in SEM systems. External storage devices such as USB drives and optical discs may also be utilized for portable or backup storage. Data storage media vary in storage capacity and read/write speeds, with larger capacity and faster access times enabling efficient storage and retrieval of large datasets generated during SEM experiments.

5.4. Image and Data Processing Software

Image and data processing software are used to analyse, enhance, and annotate SEM images and spectra. SEM software platforms provide a range of image processing and analysis tools, including contrast

adjustment, filtering, edge detection, segmentation, and measurement tools. Spectral analysis software enables qualitative and quantitative analysis of energy-dispersive X-ray spectroscopy (EDS) and other analytical data. Image and data processing software are integrated with SEM control software, allowing seamless transition between image acquisition, processing, analysis, and reporting. Customizable workflows and automation features streamline data processing and analysis tasks.

5.5. Real-Time Image and Data Display

Real-time image and data display allows users to observe SEM images and analytical results as they are acquired, enabling immediate feedback and adjustment of experimental parameters. Real-time image and data display is facilitated through dedicated software interfaces or graphical user interfaces (GUIs) integrated into SEM control software. Live image previews, spectra displays, and measurement readouts provide instant feedback on sample characteristics and experimental conditions.

5.6. Remote Access and collaboration

Remote access and collaboration capabilities allow users to access SEM images and data from remote locations, enabling collaboration, sharing, and remote operation of SEM instruments. Web-based interfaces, virtual private networks (VPNs), and remote desktop software facilitate remote access to SEM systems. Cloud-based storage and collaboration platforms enable sharing and collaboration on SEM data among multiple users and research teams.

5.7. Data Export and Documentation

Data export and documentation features enable users to export SEM images, spectra, and analytical results in various file formats for further analysis, presentation, and publication. SEM software typically supports export of images and data in standard file formats such as TIFF, JPEG, PNG, and ASCII for compatibility with external software packages and publication platforms. SEM software allows users to annotate images and spectra with descriptive metadata, scale bars, labels, and measurement annotations for improved documentation and interpretation.

5.8. Data Management and Archiving

Data management and archiving systems ensure the secure storage, organization, and long-term preservation of SEM images and data. Data management systems include database management software, digital asset management (DAM) systems, or laboratory information management systems (LIMS) for cataloging, indexing, and retrieving SEM data. Archiving solutions such as tape libraries and offsite backups ensure redundancy and disaster recovery. [34]

4.3 SCANNING TRANSMISSION ELECTRON MICROSCOPE (STEM)

Scanning Transmission Electron Microscopy (STEM) is a technique that combines the capabilities of both transmission electron microscopy (TEM) and scanning electron microscopy (SEM). It allows for high-resolution imaging and analysis of materials with atomic-scale resolution. STEM operates by passing a focused electron beam through a thin sample, and detectors positioned below the sample collect the transmitted electrons to form an image. In STEM, a finely focused electron beam scans across the sample in a raster pattern. As the beam interacts with the sample, various signals are generated, including transmitted electrons, scattered electrons, and emitted X-rays. These signals carry valuable information about the sample's composition, structure, and properties. The transmitted electrons, which pass through the sample without significant scattering, are collected by detectors positioned below the sample. These detectors play a crucial role in forming the STEM image and obtaining information about the sample's atomic structure. In Scanning Transmission Electron Microscopy (STEM), various types of detectors are used to collect and analyse electrons that have interacted with the sample. Each type of detector provides specific information about the sample's structure, composition, and properties as follows

1. Annular Dark-Field (ADF) Detector:

ADF detectors collect electrons scattered at large angles ($> \sim 100$ mrad) relative to the incident electron beam. ADF imaging is sensitive to atomic number (Z)

variations in the sample. Heavier elements scatter electrons more strongly, resulting in brighter contrast in the image. ADF imaging is particularly useful for imaging heavy elements and distinguishing between materials with different compositions

2. Annular Bright-Field (ABF) Detector:

ABF detectors collect electrons that have undergone little scattering and are transmitted through the sample without significant deflection. ABF imaging provides contrast based on variations in sample thickness and density. Thicker regions appear brighter due to increased electron scattering. ABF imaging is useful for obtaining high-resolution images of the sample's structure, revealing fine details and interfaces.

3. High-Angle Annular Dark Field(HAADF) Detector:

HAADF detectors collect electrons scattered at high angles ($> \sim 20$ mrad) relative to the incident electron beam. HAADF imaging primarily depends on the atomic number (Z) of the sample. Heavier elements scatter electrons more strongly, resulting in brighter contrast. HAADF imaging is excellent for imaging heavy elements and providing atomic-resolution images of crystalline materials, allowing the visualization of individual atomic columns.

4. Low-Angle Annular Dark Field(LAADF) Detector:

LAADF detectors collect electrons scattered at low angles ($< \sim 20$ mrad) relative to the incident electron beam. LAADF imaging enhances contrast based on differences in the atomic number (Z) of the sample. It is particularly sensitive to variations in heavy elements. LAADF imaging is useful for imaging heavy atoms in the sample, highlighting interfaces, defects, and other features with high Z contrast.

5. Energy- Dispersive X-ray Spectroscopy (EDS):

Energy-Dispersive X-ray Spectroscopy (EDS) detector in Scanning Transmission Electron Microscopy (STEM) is a powerful analytical technique used to investigate the elemental composition of materials at the Nano scale.

The components of EDS detector are

1. Solid-State Detector Crystal

At the heart of an EDS detector lies the solid-state crystal, typically composed of silicon or germanium. This crystal serves as the primary component for X-ray detection. When high-energy X-rays interact with the

crystal, they generate electron-hole pairs, leading to the production of electrical signals proportional to the energy of the incident X-rays.

2. Amplification and Signal Processing Electronics

The electrical signals generated by the solid-state crystal are relatively weak and require amplification for accurate detection and analysis. Signal amplification electronics boost the signals to measurable levels while maintaining their integrity. Additionally, signal processing electronics perform functions such as pulse shaping, filtering, and digitization, ensuring that the detected signals can be processed and analysed effectively.

3. Multi-Channel Analyser(MCA)

The multichannel analyser is a crucial component responsible for converting the analog signals from the detector into digital form. It segments the energy spectrum into discrete channels, with each channel corresponding to a specific energy range. The MCA facilitates the generation of spectra, which represent the distribution of X-ray energies emitted by the sample.

4. Preamplifier and cooler:

To minimize noise and enhance signal-to-noise ratio, EDS detectors often incorporate preamplifiers positioned close to the detector crystal. These preamplifiers immediately amplify the weak signals generated by X-ray interactions before they travel further through the signal processing chain. Additionally, some detectors feature cooling mechanisms to maintain stable operating temperatures, reducing thermal noise and enhancing detector performance.

The detection of X-rays in EDS is based on the principle of energy-dispersive spectroscopy. When an incident electron beam interacts with the sample, it causes inner-shell ionization of atoms, leading to the emission of characteristic X-rays as the excited electrons transition to lower energy states. Each element produces X-rays with unique energies corresponding to its atomic structure. The EDS detector measures the energies of these X-rays, allowing for the identification and quantification of the elements present in the sample. [38]

The common applications of EDS in STEM are as follows

1. Element Mapping

Elemental mapping is a technique used to spatially resolve the distribution of elements within a sample. In STEM-EDS, elemental maps are generated by acquiring EDS spectra at each pixel of an image while scanning the electron beam across the sample. The intensity of characteristic X-rays emitted by each element is recorded, enabling the construction of maps showing the spatial distribution of elements. Elemental mapping provides valuable information about the elemental composition and distribution within materials, facilitating the study of phase segregation, diffusion, and elemental interactions.

2. Phase Identification

Phase identification in STEM-EDS involves determining the chemical composition of distinct phases within a sample. By analysing the characteristic X-ray spectra acquired from different regions of the sample, researchers can identify the elements present and their relative abundances. Phase identification is particularly important in materials science and geology for characterizing complex microstructures, identifying phases with different crystal structures or chemical compositions, and elucidating phase transformations and reactions under various conditions.

3. Quantitative Analysis

Quantitative analysis in STEM-EDS aims to determine the elemental composition of a sample and quantify the relative concentrations of different elements. This is achieved by comparing the intensities of characteristic X-ray peaks in the acquired spectra with known standards or reference materials. Calibration curves or matrix correction algorithms are used to account for factors such as X-ray absorption, fluorescence, and detector efficiency, enabling accurate quantification of elemental concentrations. Quantitative analysis is essential for characterizing material compositions, assessing impurity levels, and studying elemental segregation or diffusion processes.

4. Defect Analysis

Defect analysis using STEM-EDS involves examining defects, such as vacancies, dislocations, grain boundaries, and interfaces, and investigating their chemical composition and spatial distribution. By acquiring high-

resolution STEM images and corresponding EDS spectra from defect sites, researchers can identify the elemental signatures associated with specific defects. Defect analysis provides insights into the formation mechanisms, stability, and effects of defects on material properties, offering valuable information for materials design, processing, and optimization.

5. Chemical Speciation

Chemical speciation refers to the identification and characterization of chemical species or compounds within a sample. In STEM-EDS, chemical speciation can be achieved by analysing the X-ray spectra to identify characteristic peaks corresponding to specific chemical bonds or coordination environments. Chemical speciation is essential for understanding chemical reactions, surface chemistry, and catalytic processes in diverse scientific fields.

6. Electron Energy Loss Spectroscopy(EELS)

Electron Energy Loss Spectroscopy (EELS) is a powerful analytical technique used to investigate the elemental composition, chemical bonding, and electronic structure of materials at the nanometre scale. EELS rely on the interaction of high-energy electrons with a sample to probe its composition and electronic structure. When high-energy electrons pass through a material, they lose energy due to interactions with the sample's electrons. This energy loss is characteristic of the material's composition and electronic properties, providing valuable information about its structure and bonding. The energy loss spectrum obtained from EELS contains peaks corresponding to various energy losses associated with different electronic transitions within the sample. By analysing these peaks elemental composition, chemical state, and bonding configuration of the material under investigation can be determined. EELS in STEM find wide range of applications including elemental mapping, chemical bonding analysis, electronic structure studies and characterisation of Nano materials.[39]

CHAPTER 5

RESULTS AND DISCUSSION

5.1. TENSILE TEST ANALYSIS

(a) Mg-0.3%wtZr alloy

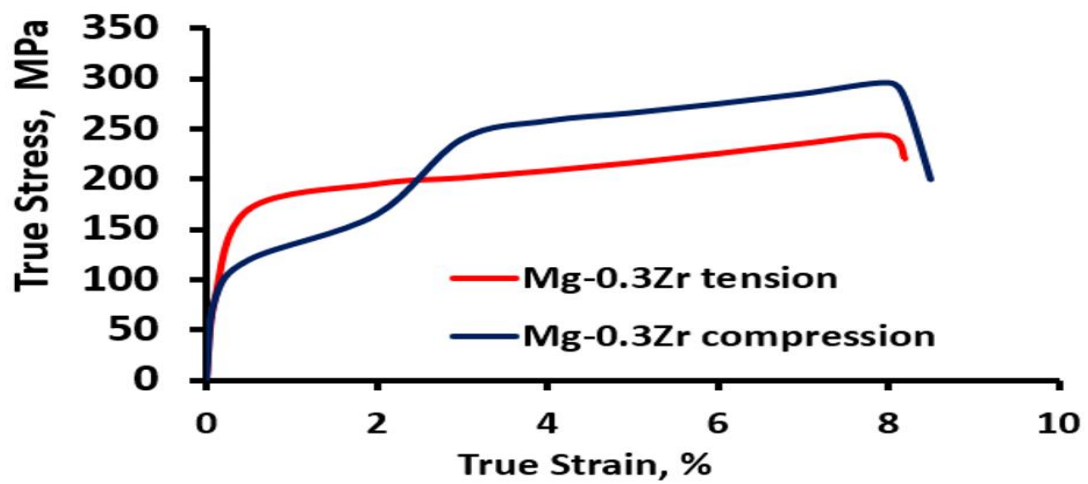


Fig 5.1: Stress-strain plot of Mg-0.3%wtZr alloy

- Yield stress(tension)- 165 MPa
- Yield stress(compression)-115 MPa
- Elongation %(tension)-7.9
- Elongation %(Compression)-8.2

(b) Mg-0.3%wtSn alloy

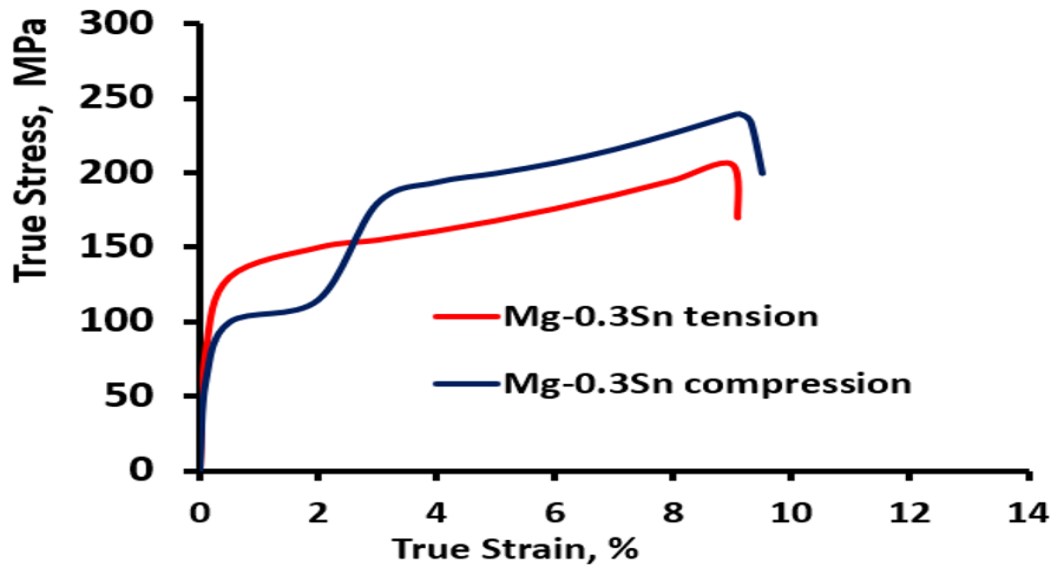


Fig 5.2: Stress-strain plot of Mg-0.3%wtSn alloy

- Yield stress(tension)- 125 MPa
- Yield stress(compression)-95 MPa
- Elongation %(tension)-9.1
- Elongation %(Compression)-9.3

(c) Mg-0.3%wtZr-0.3%wtSn alloy

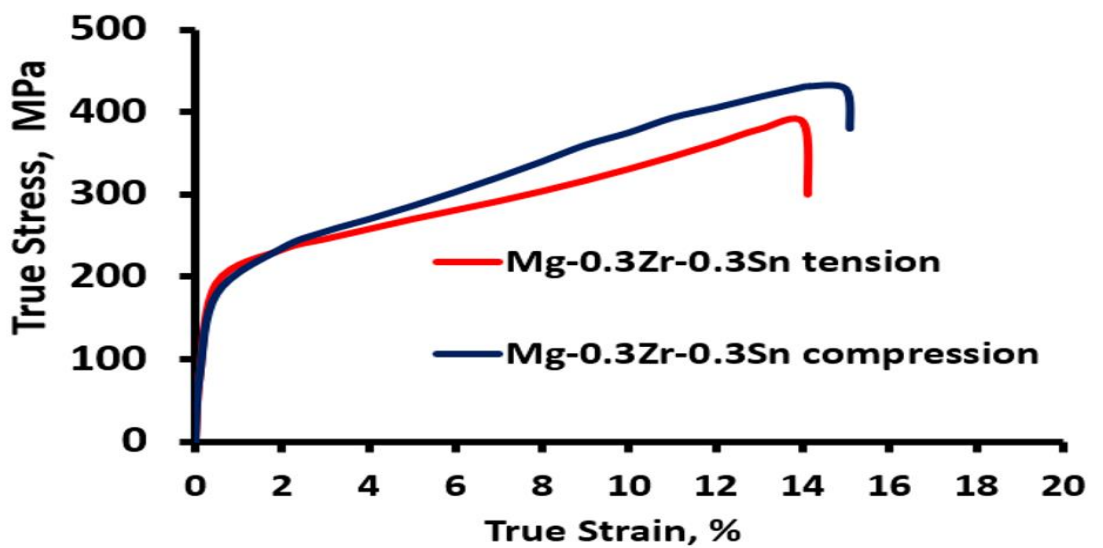


Fig 5.3: Stress-strain plot of Mg-0.3%wtZr-0.3%wtSn alloy

- Yield stress(tension)- 188 MPa
- Yield stress(compression)-175 MPa
- Elongation %(tension)-14.1
- Elongation %(Compression)-15.1

As the primary motive of this research work is to weaken the basal structure in order to activate more slip systems in non- basal planes and improve the ductility and formability of magnesium alloy, it is important to analyse the Tension-Compression Yield asymmetry. Tension-compression yield asymmetry refers to the difference in mechanical behaviour between tensile and compressive loading. The factors that contribute to tension-compression yield asymmetry are

- Basal Slip Systems- The HCP crystal structure of magnesium alloys provide multiple slip systems for plastic deformation with the basal slip system(shearing along the basal plane) being the most favoured. In tension, the basal slip is dominant which makes Mg alloys more ductile in tension. In compression, prismatic and pyramidal slip systems become more active which are less favourable for plastic deformation leading to a higher yield stress and less ductility.
- Alloy composition- The presence of alloying elements significantly impacts the yield asymmetry. Different alloying element can affect the activity of slip systems, texture and other microstructural features, leading to variations in yield stress and deformation behaviour.
- Texture and grain morphology- The preferred orientation of grains in magnesium alloys can lead to variations in yield asymmetry which is due to the methods of processing the alloys like rolling and extrusion. This variation in texture will be an addition to the anisotropic property of Magnesium (HCP Structure) leading to increased tension-compression yield asymmetry [6].

Thus the tension-compression yield asymmetry can be succeeded by modification of alloy composition and undertaking optimum severe plastic deformation techniques.

From the results, it should be noted that **Mg-0.3%wtZr-0.3%wtSn alloy** perform better in terms of improvement in elongation and reducing the yield asymmetry.

5.1.1. ELONGATION (%)

- Compared to Mg-0.3% wtZr alloy ,
Mg-0.3% wtZr-0.3% wtSn alloy show 78.48% increase in elongation in tension and 84.146 % increase in elongation in compression
- Compared to Mg-0.3Sn alloy,
Mg-0.3% wtZr-0.3% wtSn alloy show 54.95% increase in elongation in tension and 62.36 % increase in elongation in compression

5.1.2. YIELD STRESS

- Compared to Mg-0.3% wtZr alloy ,
Mg-0.3% wtZr-0.3% wtSn alloy show 13.93% increase in yield stress in tension and 52.174 % increase in yield stress in compression
- Compared to Mg-0.3% wtSn alloy,
Mg-0.3% wtZr-0.3% wtSn alloy show 50.40% increase in elongation in tension and 84.21 % increase in elongation in compression

5.1.3. YIELD RATIO

Yield ratio is a dimensionless ratio of yield strength in tension to yield strength in compression. The yield ratio is significant for

- Formability assessment-
Formability assessment is a crucial aspect of material processing, particularly in manufacturing processes like sheet metal forming, where the ability of a material to deform without fracture or defects is essential. It involves evaluating the material's behaviour under various forming conditions to determine its suitability for specific manufacturing processes. A low yield ratio suggests that a material have good formability because its yield strength in tension and compression are relatively close.
- Anisotropy Characterization- Anisotropy refers to the directional dependence of material properties, where the properties vary with the direction of measurement relative to the material's microstructure or processing history.

Anisotropic materials exhibit different mechanical behaviours, such as stiffness, strength, and ductility, in different directions. The yield ratio quantifies the anisotropic behaviour of material by comparing its yield strength in different directions. A high yield ratio indicates that the material's yield strength in tension is significantly different from its yield strength in compression, which means the material is anisotropic in terms of yield behaviour.

- Strain path dependency- Strain path dependency refers to the phenomenon where the mechanical behaviour of a material depends on its deformation history or the path followed during loading and unloading cycles. This behaviour is particularly significant in materials subjected to complex loading conditions or multiple forming operations. Materials with a low yield ratio are less sensitive to changes in strain path, making them more versatile for various forming operations.
- Material selection- Material selection is a critical decision-making process in engineering design, involving the identification and evaluation of suitable materials for specific applications based on their properties, performance requirements, and cost considerations. For parts requiring extensive plastic deformation, materials with a low yield ratio are preferred because they are less likely to crack or fail during the forming process. Conversely, materials with a high yield ratio may be suitable for applications that do not involve extensive forming.
- Predicting spring-back- Spring back, also known as elastic recovery or elastic deformation, is a phenomenon observed in materials undergoing plastic deformation followed by unloading. It refers to the tendency of a material to partially return to its original shape or dimensions after the removal of external loads, due to the release of stored elastic energy. Low yield ratio material is less prone to spring-back making them favourable for applications where tight tolerances are essential.

Here,

Alloy	Yield stress(tension), MPa	Yield stress (Compression), MPa	Yield Stress Ratio
Mg-0.3%wtZr	165	115	1.43
Mg-0.3%wtSn	125	95	1.31
Mg-0.3%wtZr-0.3%wtSn	188	175	1.07

Mg-0.3% wtZr-0.3%wtSn has least value of yield stress ratio indicating better ductile material as compared to Mg-0.3% wtZr and Mg-0.3%wtSn.

5.2. EBSD ANALYSIS

5.2.1. Mg-0.3%wtZr alloy

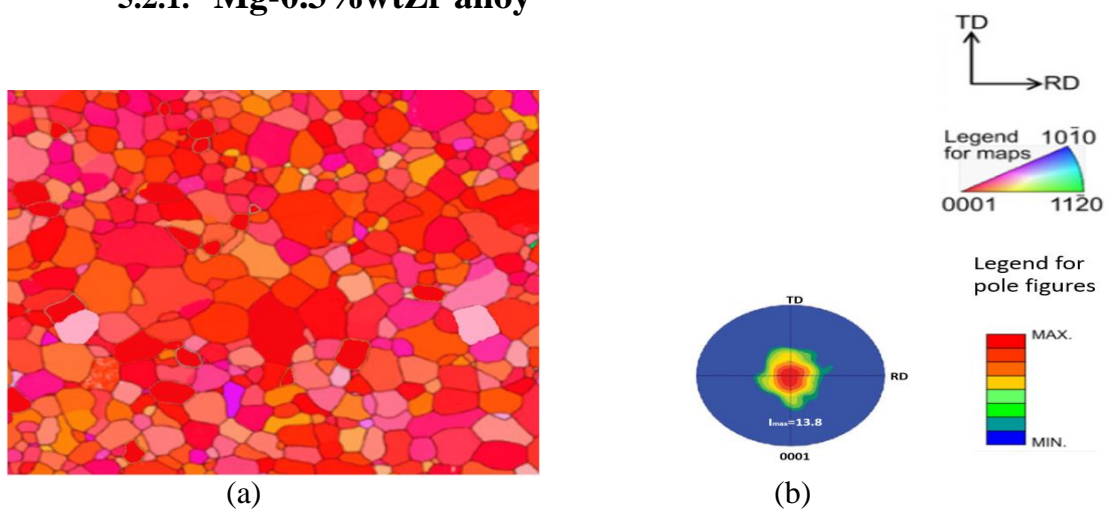


Fig 5.4: (a) EBSD Inverse Pole Figure (IPF) Maps (b) Pole figures of Mg-0.3%wt Zr sample

Hot rolling at 300°C + Annealed at 250°C for 20 minutes

Average grain size $\sim 18 \mu\text{m}$

5.2.2. Mg-0.3%wtSn alloy

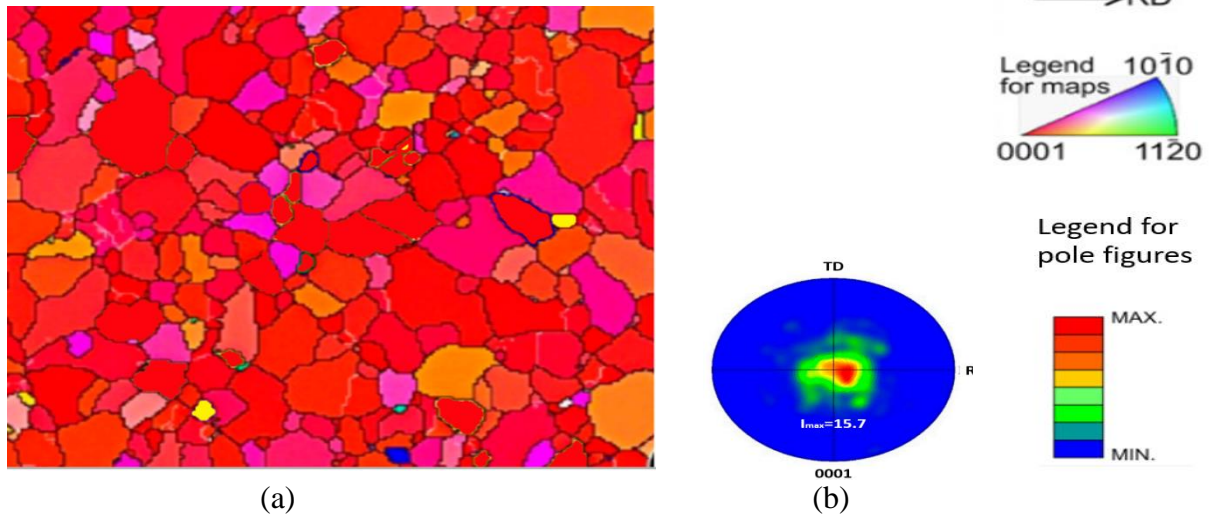


Fig 5.5: EBSD Inverse Pole Figure (IPF) Maps (b) Pole figures of Mg-0.3%wt Sn sample

Hot rolling at 300°C + Annealed at 250°C for 20 minutes

Average grain size $\sim 25 \mu\text{m}$

5.2.3. Mg-0.3%wtZr-0.3%wtSn alloy

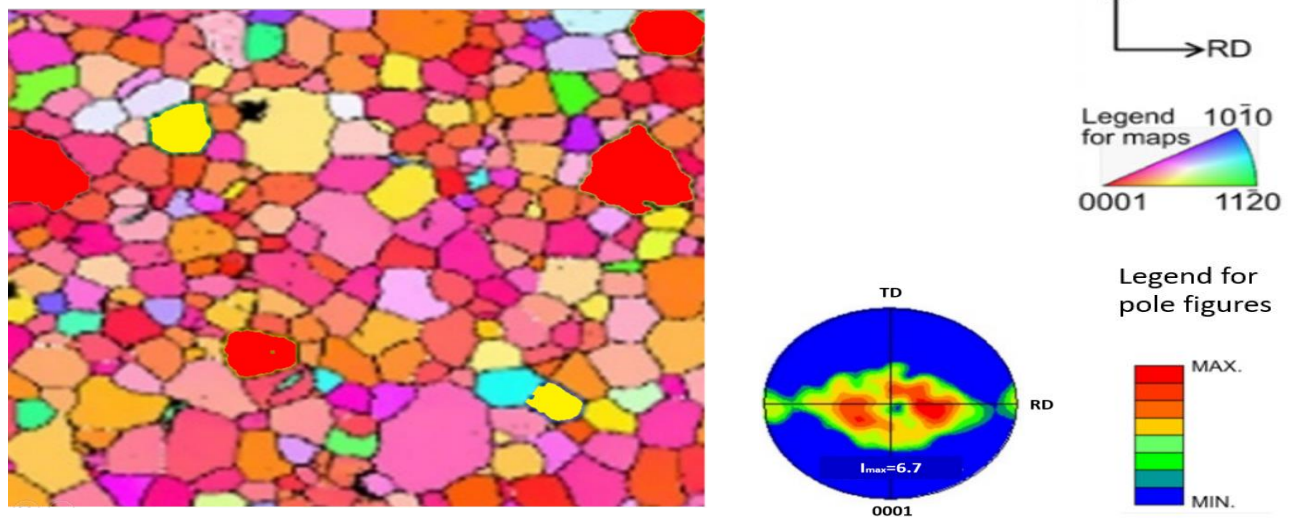


Fig 5.6: EBSD Inverse Pole Figure (IPF) Maps (b) Pole figures of Mg-0.3%wtZr-0.3%wt Sn sample

Hot rolling at 300°C + Annealed at 250°C for 20 minutes

Average grain size ~14 μm

In EBSD maps, each crystallographic orientation is assigned a unique colour. This colour mapping is often represented using a colour wheel, where different hues correspond to different crystallographic orientations. From the above three figures it can be deduced that

- Most of the crystal orientations are towards [0001] in case of Mg-0.3%wtZr and Mg-0.3%wtSn indicating it to be more textured. If a material is more textured it indicates that it will exhibit anisotropic behaviour thus causing huge yield asymmetry as material tend to behave in a biased manner during the application of load due to crystal orientation in a particular direction. Also due to less segregation effect, the material is less randomized. This implies less weakening of basal structure, limited slip systems and limited ductility.
- In case of Mg-0.3%wtZr-0.3%wtSn the grains are oriented in different direction. Due to high randomisation it exhibits isotropic behaviour and yield asymmetry is reduced. Also pyramidal slip systems are activated due to randomization contributing to enhanced ductility. Both Zr and Sn contribute to more segregation effects thus making it more randomised.
- Also the average grain size of Mg-0.3%wtZr-0.3%wtSn is less than that of Mg-0.3%wtZr and Mg-0.3%wtSn indicated more grain boundaries and these interfaces hinder the movement of dislocations, resulting in enhanced strength.
- Thus Mg-0.3%wtZr-0.3%wtSn contributes to more ductility and strength as compared to Mg-0.3%wtZr and Mg-0.3%wtSn.

5.3. STEM ANALYSIS

In this analysis STEM-LAADF with Camera Length (CL) of 200 mm is employed to determine the diffraction contrast and STEM-HAADF with Camera Length (CL) of 80 mm is employed to determine the Z-Contrast.

5.3.1. Mg-0.3%wtZr alloy

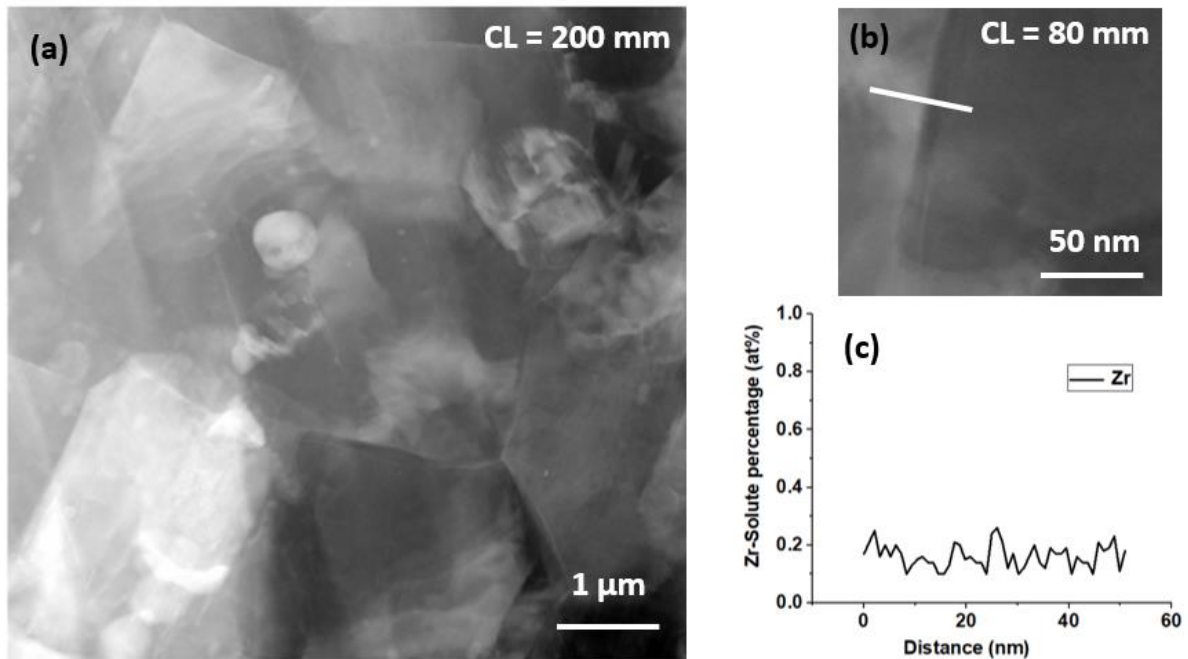


Fig 5.7:

(a)STEM-LAADF image acquired with CL = 200 mm showing the diffraction contrast from the different grains in Mg-0.3%wtZr alloy (b) STEM-HAADF image showing the grain boundary across which the STEM-EDS line profile analysis was conducted in Mg-0.3%wtZr alloy(c) STEM-EDS line profile plot showing no peak from grain boundary which indicates no grain boundary segregation of Zr.

When an incident electron beam interacts with the periodic arrangement of atoms in a crystalline sample, it undergoes diffraction, analogous to the diffraction of light waves by a grating. The scattered electrons form a diffraction pattern, which contains information about the spatial distribution of

atoms and their arrangement within the crystal lattice. The intensity of the diffraction spots in the pattern depends on factors such as the atomic number of the atoms, the orientation of the crystal, and the wavelength of the incident electrons. In diffraction contrast imaging, the interaction of the incident electron beam with the crystal lattice results in the formation of bright and dark contrast features in the image. Bright contrast regions correspond to areas where the scattered electrons have experienced constructive interference, leading to higher electron intensity at those positions. This constructive interference occurs when the scattered waves from adjacent atomic planes of the crystal lattice reinforce each other, resulting in an increase in intensity in the diffraction pattern.

Several factors influence the appearance of bright contrast in diffraction contrast imaging:

Crystal Orientation: -

The orientation of the crystal relative to the incident electron beam determines the angles at which diffraction occurs, affecting the intensity and spatial distribution of bright contrast features.

Atomic Arrangement: -

The atomic arrangement within the crystal lattice dictates the spacing between atomic planes and the angles at which diffraction peaks occur. Variations in atomic arrangement, such as defects, dislocations, or grain boundaries, can alter the intensity and position of bright contrast regions in the image.

Electron Beam Conditions: -

The energy, coherence, and intensity of the incident electron beam influence the degree of electron scattering and the formation of diffraction patterns. Higher-energy electrons can penetrate deeper into the specimen, interacting with a larger number of atoms and generating stronger diffraction contrast.

Bright contrast features in diffraction contrast images provide valuable information about the crystalline structure (like grain boundaries & Dislocations) and defects within materials. However, diffraction contrast alone may not be sufficient for analysing segregation because it primarily provides structural information rather than compositional information. While it can reveal the presence of certain defects associated with segregation, such as

stacking faults or precipitates, it cannot directly quantify the distribution of specific elements within the material. Z-contrast imaging, on the other hand, utilizes the differences in atomic number (Z) between different elements in a material. It is typically achieved using techniques such as high-angle annular dark-field (HAADF) scanning transmission electron microscopy (STEM). In Z-contrast imaging, the intensity of the electron signal is directly proportional to the atomic number of the elements in the sample. This allows for the visualization and quantification of compositional variations, including segregation of different elements within the material. Z-contrast imaging can provide detailed information about the distribution of segregated elements at atomic-scale resolution, which is crucial for understanding the effects of segregation on material properties.

In this case EDS spectroscopy is conducted across the grain boundary of Mg-0.3%wtZr alloy in order to determine whether any segregation has occurred. The grain boundary region is chosen for segregation analysis for the following reasons,

High energy sites: - Grain boundaries are regions of high energy compared to the interior of the grains. This higher energy makes them more chemically reactive and thermodynamically favourable sites for the segregation of impurity atoms or solute elements.

Lattice strain: -

At grain boundaries, the crystal lattice is disrupted and distorted to accommodate the change in orientation between neighbouring grains. This lattice strain creates local distortions and defects, making grain boundaries attractive sites for the trapping and segregation of foreign atoms.

Enhanced diffusion: -

Diffusion of atoms or ions is often enhanced at grain boundaries compared to the bulk material due to the presence of vacancies, dislocations, and other defects. This enhanced diffusion facilitates the migration of solute atoms towards grain boundaries, where they can accumulate and segregate.

Thermodynamic driving force: -

Segregation to grain boundaries can be driven by thermodynamic factors such as minimizing the system's free energy. For example, if the segregation of

certain elements reduces the overall free energy of the system, it will be energetically favourable for these elements to concentrate at grain boundaries.

Stress effects: -

Grain boundaries can act as sites for stress concentration, particularly under mechanical loading. Segregation of certain elements to grain boundaries can influence the mechanical properties of the material, such as its strength, ductility, and fracture toughness. Since no peak is shown in the grain boundary region of Mg-0.3%wtZr alloy, it shows no segregation has occurred. Binary alloys often exhibit fewer segregation effects because of the following factors,

Simplicity of the system: -

Binary alloys have a simpler composition compared to ternary alloys, with fewer alloying elements and phase interactions. This simplicity reduces the complexity of segregation phenomena and facilitates a more uniform distribution of alloying elements within the microstructure.

Limited number of phases: -

Binary alloys typically form fewer phases compared to ternary alloys, resulting in a narrower range of phase equilibria and segregation behaviours. The absence of multiple phases with distinct compositions reduces the opportunities for segregation at phase boundaries and interfaces.

Enhanced solid solubility: -

Binary alloys with similar atomic sizes and chemical affinities often exhibit enhanced solid solubility, leading to more homogeneous mixing of alloying elements within the lattice. The absence of significant phase separation tendencies reduces the likelihood of segregation at grain boundaries or defects.

Reduced diffusion paths: -

Binary alloys have simpler diffusion pathways compared to ternary alloys, with fewer atomic species diffusing through the lattice. This results in more uniform diffusion profiles and reduced segregation effects, especially under equilibrium or near-equilibrium conditions.

6.3.2. Mg-0.3%wtSn alloy

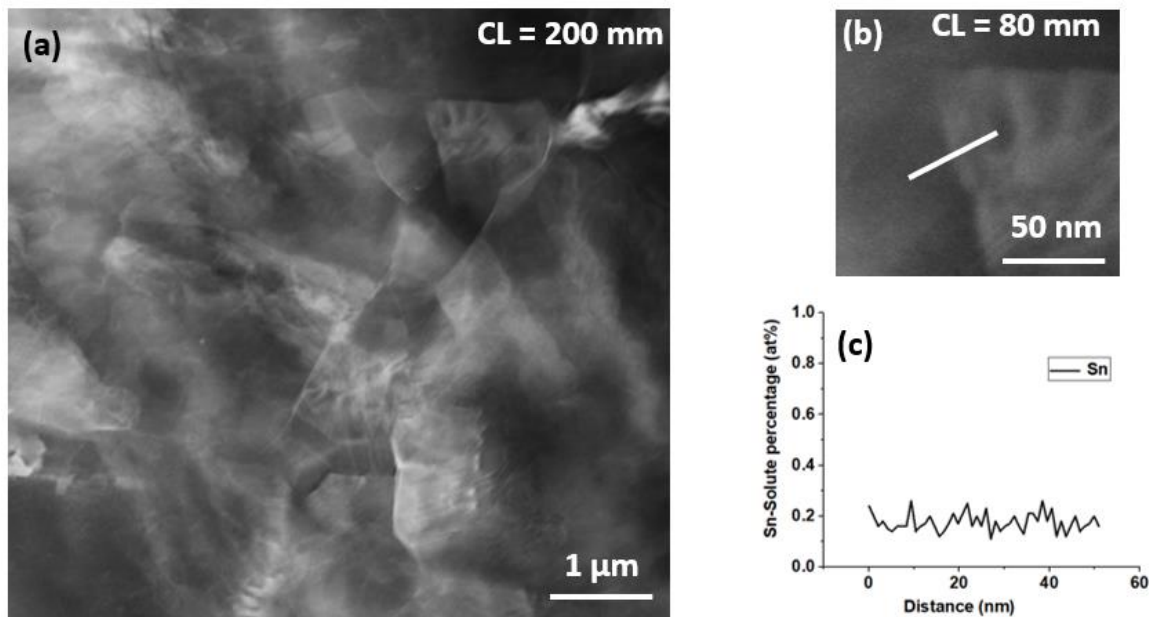


Fig 5.8:

(a) STEM-LAADF image acquired with CL = 200 mm showing the diffraction contrast from the different grains in Mg-0.3%wtSn alloy.(b) STEM-HAADF image showing the grain boundary across which the STEM-EDS line profile analysis was conducted in Mg-0.3%wtSn alloy.(c) STEM-EDS line profile plot showing no peak from grain boundary which indicates no grain boundary segregation of Sn.

Similar to Mg-0.3%wtZr, Mg-0.3%wtSn alloy did not show any segregation effect due to the same binary alloy reasons. Yet Sn has lesser size compared to Zr and less stacking fault energy but still it does not possess sufficient potential as in the case of ternary alloys for segregation to take place. Reduced diffusion paths and enhanced solubility overshadow the size factor thus preventing the segregation effects in Mg-0.3%wtSn alloy.

Segregation can occur in binary alloys for the following reasons,

Atomic size misfit: -

Differences in atomic size between the two alloying elements can lead to lattice strain and distortions, promoting segregation at interfaces and defects to minimize elastic

energy. Larger atoms may segregate preferentially to sites with higher coordination numbers, such as grain boundaries or dislocations, while smaller atoms may diffuse more readily into the bulk lattice.

Thermodynamic driving forces: -

Segregation in binary alloys is influenced by the Gibbs free energy of mixing, which governs the tendency of alloying elements to form solid solutions or phase separate. Positive enthalpy of mixing (ΔH_{mix}) favours phase separation, leading to the formation of distinct phases with different compositions. Negative ΔH_{mix} promotes solid solution formation, where alloying elements are homogeneously distributed within the lattice.

Kinetic factors: -

Diffusion kinetics plays a crucial role in determining the extent and rate of segregation in binary alloys. Rapid diffusion of alloying elements along grain boundaries or interfaces can lead to segregation, especially under non-equilibrium conditions such as rapid cooling or solidification.

But all the above factors are not sufficient in this case to promote segregation effects.

6.3.3. Mg-0.3%wtZr-0.3%wtSn alloy

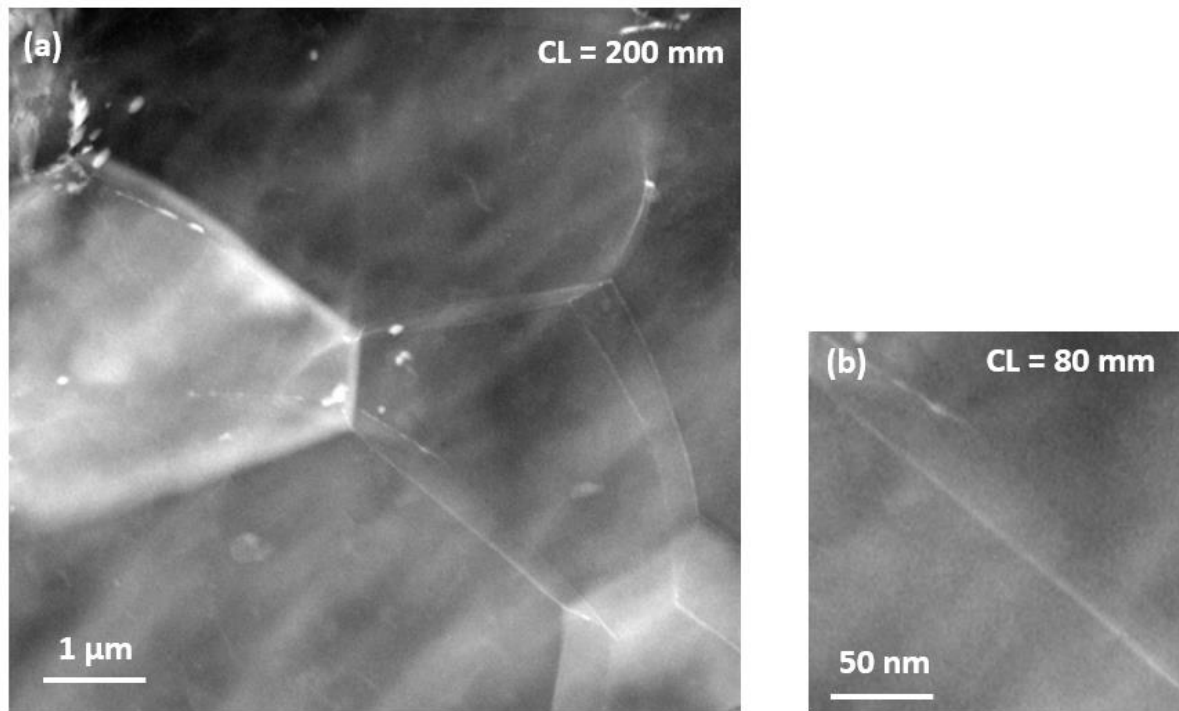


Fig 5.9:

(a) STEM-LAADF image acquired with CL = 200 mm showing the diffraction contrast from the different grains in Mg-0.3%wtZr-0.3%wtSn alloy.(b)STEM-HAADF image showing the grain boundary across which the STEM-EDS line profile analysis was conducted in Mg-0.3%wtZr-0.3%wtSn alloy.

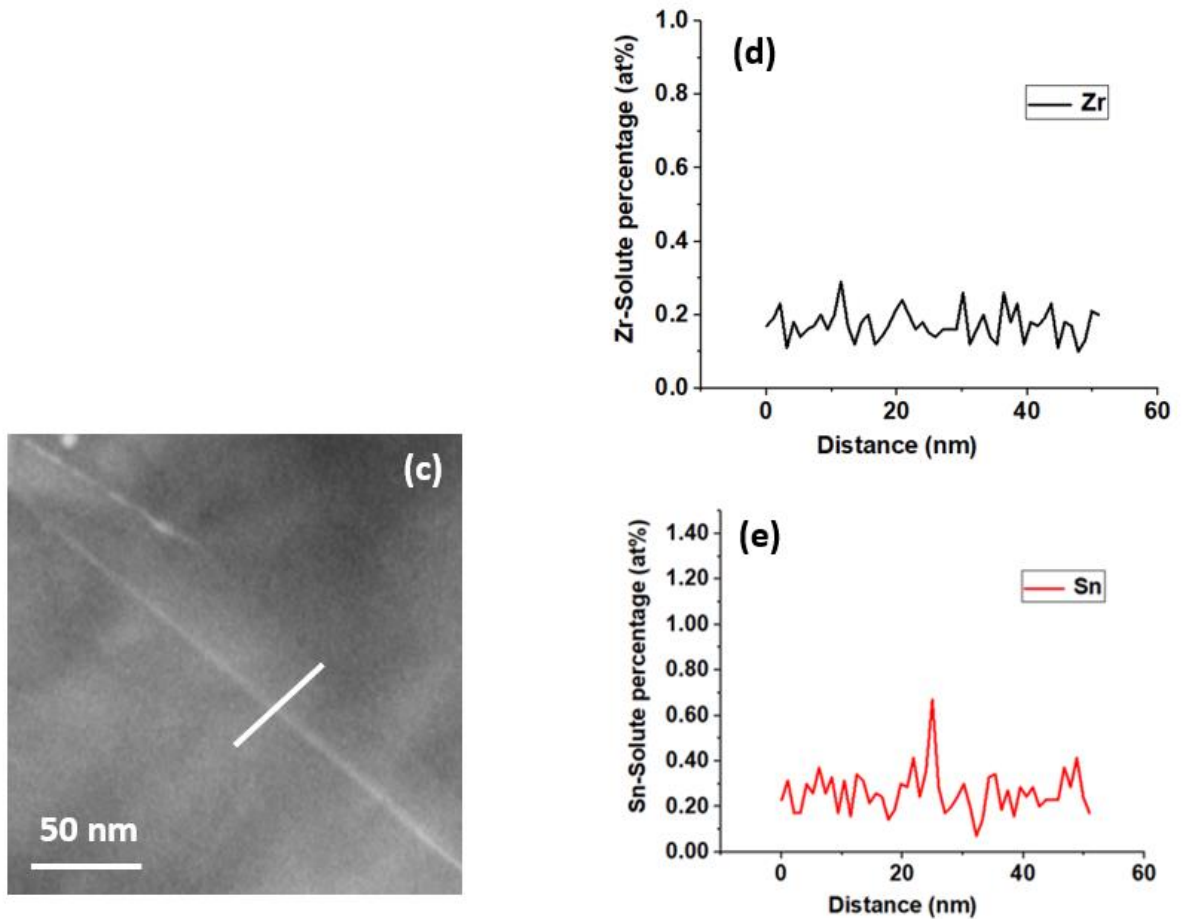


Fig 5.10:

(c) STEM-HAADF image showing the grain boundary across which the STEM-EDS line profile analysis was conducted in Mg-0.3%wtZr-0.3%wtSn alloy.(d) STEM-EDS line profile plot showing no peak from grain boundary which indicates no grain boundary segregation of Zr.(e) STEM-EDS line profile plot showing peak from grain boundary which indicates grain boundary segregation of Sn. (Atomic number of Sn > Atomic number of Zr)

Mg-0.3%wtZr-0.3%wtSn alloy shows segregation phenomenon compared to Mg-0.3%wtZr and Mg-0.3%wtSn because of the following reasons,

Diffusion along multiple paths: -

In ternary alloys, atoms can diffuse along multiple paths, including interstitial sites, grain boundaries, and interfaces between different phases. The presence of multiple diffusion pathways increases the likelihood of solute atoms migrating to specific regions with favourable energetics, leading to enhanced segregation effects. Additionally, the interaction between different alloying elements may influence the diffusion kinetics and pathways, further contributing to segregation phenomena. The kinetics of diffusion in ternary alloys may differ significantly from binary systems due to the interaction between multiple elements and phases. Complex diffusion mechanisms, such as cooperative diffusion, coupled diffusion, or competitive diffusion, can occur in ternary alloys, affecting the rate and extent of segregation. The presence of multiple diffusion mechanisms and competing interactions complicates the prediction and control of segregation behaviour in ternary systems.

Wide range of atomic interactions: -

The combination of different atomic interactions results in synergistic effects that promote segregation. The interaction between atomic bonding and diffusion influences the mobility of solute atoms and their affinity for specific crystallographic sites. This synergism accelerates the segregation process, leading to the formation of distinct phases or regions within the alloy. Atomic interactions dictate the site preference of solute atoms within the alloy lattice. In ternary systems, the energetics of atomic bonding determines whether solute atoms preferentially occupy specific lattice sites or interstitial positions. This site preference influences the spatial distribution of solute atoms and contributes to segregation phenomena. The kinetics of atomic interactions influences the rate at which segregation occurs in ternary alloys. Factors such as diffusion coefficients, nucleation rates, and growth kinetics determine the kinetics of phase transformations and the evolution of segregated microstructures.

Thermodynamic driving forces: -

The chemical potential of each element in a ternary alloy influences its tendency to segregate. Variations in chemical potential drive the diffusion of atoms, leading to the formation of composition gradients within the microstructure. Differences in chemical potential between the constituent elements result in segregation at interfaces and grain boundaries. Interfacial energies at phase boundaries dictate the equilibrium shapes and stability of phases in ternary alloys. Variations in interfacial energies between different phases can promote segregation at specific interfaces, leading to the formation of complex microstructures with segregated regions. Entropy effects, such as mixing entropy and configurational entropy, influence the distribution of atoms in ternary alloys. The entropy of mixing governs the tendency of atoms to distribute uniformly or segregate based on their chemical interactions and spatial arrangements. Deviations from ideal mixing behaviour can lead to segregation phenomena.

Lattice strain or distortion: -

One of the primary contributors to lattice strain in ternary alloys is the atomic size mismatch between the constituent elements. Each element has a specific atomic radius, and when combined in an alloy, variations in atomic size can disrupt the regular lattice arrangement. Ternary alloys with significant atomic size mismatches experience lattice distortion, leading to the formation of strained regions within the crystal lattice. The chemical affinity between elements in a ternary alloy influences their coordination and bonding within the crystal lattice. Elements with different electro negativities or valence states may form bonds of varying strengths, resulting in lattice strain. Chemical interactions between the elements can lead to distortions in the lattice structure, affecting its stability and properties. Lattice strain can promote segregation at grain boundaries and interfaces within ternary alloys. Variations in atomic arrangement and bonding at these interfaces create preferential sites for the accumulation of solute atoms, leading to segregation. The presence of lattice strain enhances the energy of these interfaces, further driving the segregation of solute atoms to reduce the overall system energy. Lattice strain

can facilitate the diffusion of atoms within ternary alloys by providing preferential pathways for atomic motion. Local distortions in the lattice structure create gradients in chemical potential, driving the migration of solute atoms along the strain field. This strain-assisted diffusion enhances segregation phenomena by accelerating the redistribution of solute atoms within the material.

In Mg-0.3%wtZr-0.3%wtSn, Sn undergoes segregation compared to Zr because of the following reasons,

Atomic Size: -

Size of Sn (1.4Å) is smaller as compared to Zr (1.55Å) as Sn has more protons in the nucleus pulling more electrons closer thus less atomic size compared to Zr. Atoms with less size segregate easily across the grain boundary region as it possesses higher diffusion rates and can readily overcome interatomic or intermolecular forces.

Electronegativity: -

Electronegativity is a measure of the tendency of an atom to attract a shared pair of electrons towards itself when it forms a chemical bond with another atom. Electronegativity of Sn (1.96) is higher than that of Zr(1.33) enabling it to form better bond formation thus promoting segregation phenomenon.

Diffusion Coefficient: -

The diffusion coefficient describes the rate at which atoms move through a material. Elements with higher diffusion coefficients are more likely to diffuse and segregate within an alloy. In the Mg-Zr-Sn system, the diffusion coefficient of tin (Sn) is always higher compared to magnesium (Mg) and zirconium (Zr) , facilitating its segregation within the alloy over time.

Stacking fault energy: -

Stacking Fault Energy (SFE) is a measure of the energy required to create a fault in the crystal lattice of a material. Alloys with low stacking fault energy

tend to have higher propensity for segregation. In the Mg-Zr-Sn system, the stacking fault energy of tin (Sn) is lower compared to magnesium (Mg) and zirconium (Zr), making it more prone to segregation within the alloy.

Thus out of three alloys of Mg-0.3%wtZr, Mg-0.3%wtSn, Mg-0.3%wtZr-0.3%wtSn, the ternary alloy Mg-0.3%wtZr-0.3%wtSn shows better segregation thus more randomization and weakening of basal structure promoting better ductility and formability.

CHAPTER 7

CONCLUSION

In this project, Mg-0.3%wtZr, Mg-0.3%wtSn and Mg-0.3%wtZr-0.3%wtSn alloys were synthesized by stir casting process, processed by hot rolling technique at 573 K and annealed at 523 K for 20 min successfully.

1. Tension and Compression studies show that Mg-0.3%wtZr and Mg-0.3%wtSn alloys exhibit high yield asymmetry behaviour, whereas Mg-0.3%wtZr-0.3%wtSn alloy exhibits reduced yield asymmetry behaviour.
2. SEM-EBSD analysis shows that Mg-0.3%wtZr and Mg-0.3%wtSn alloys exhibit sharp basal texture, whereas Mg-0.3%wtZr-0.3%wtSn alloy exhibits weakened basal texture.
3. STEM-EDS analysis shows that segregation did not occur in Mg-0.3%wtZr and Mg-0.3%wtSn alloys exhibiting sharp basal texture, whereas Sn segregation is observed in Mg-0.3%wtZr-0.3%wtSn alloy.
4. The weakened basal texture in Mg-0.3%wtZr-0.3%wtSn alloy is due the Sn segregation, which consequently could lead to the reduction in yield asymmetry behaviour.

Thus the alloy composition Mg-0.3%wtZr-0.3%wtSn emerges as the superior choice when evaluating formability and ductility, outperforming its counterparts Mg-0.3%wtSn and Mg-0.3%wtZr.

CHAPTER 9

REFERENCES

1. Jung, Y. G., Yang, W., Kim, Y. J., Kim, S. K., Yoon, Y. O., Lim, H. K., & Kim, D. H. (2021, September 1). *Effect of Ca addition on the microstructure and mechanical properties of heat-treated Mg-6.0Zn-1.2Y-0.7Zr alloy*. Journal of Magnesium and Alloys; Elsevier BV.
2. Yu, Z., Tang, A., He, J., Gao, Z., She, J., Liu, J., & Pan, F. (2018, February 1). *Effect of high content of manganese on microstructure, texture, and mechanical properties of magnesium alloy*. Materials Characterization; Elsevier BV.
3. Zhao, T., Hu, Y., He, B., Zhang, C., Zheng, T., & Pan, F. (2019, September 1). *Effect of manganese on microstructure and properties of Mg-2Gd magnesium alloy*. Materials Science and Engineering A-structural Materials Properties Microstructure and Processing; Elsevier BV.
4. Wang, H. L., Wang, G., Hu, L., Wang, Q., & Wang, E. (2011, August 1). *Effect of hot rolling on grain refining and mechanical properties of AZ40 magnesium alloy*. Transactions of Nonferrous Metals Society of China; Elsevier BV.
5. You, S., Huang, Y., Kainer, K. U., & Hort, N. (2017, September 1). *Recent research and developments on wrought magnesium alloys*. Journal of Magnesium and Alloys; Elsevier BV.
6. Park, S. H., Lee, J. H., Moon, B. G., & You, B. S. (2014). Tension–compression yield asymmetry in as-cast magnesium alloy. *Journal of Alloys and Compounds*, 617, 277–280.
7. Davis, A., Robson, J., & Turski, M. (2019). Reducing yield asymmetry and anisotropy in wrought magnesium alloys – A comparative study. *Materials Science and Engineering: A*, 744, 525–537. Şevik, H., Açıkgöz, Ş., & Kurnaz, S. C. (2010). The effect of tin addition on the microstructure and mechanical

- properties of squeeze cast AM60 alloy. *Journal of Alloys and Compounds*, 508(1), 110–114.
8. Joy, D., Aravindakshan, R., & Varrma, N. S. (2021). Effect of Zirconium additions on microstructure and mechanical properties of hot rolled Al-Mg alloys. *Materials Today: Proceedings*, 47, 5098–5103.
 9. Tian, J., Deng, J., Zhou, Y., Chang, Y., Liang, W., & Ma, J. (2023). Slip behavior during tension of rare earth magnesium alloys processed by different rolling methods. *Journal of Materials Research and Technology*, 22, 473–488.
 10. Mansoor, P., & Dasharath, S. (2021). A review paper on magnesium alloy fabricated by severe plastic deformation technology and its effects over microstructural and mechanical properties. *Materials Today: Proceedings*, 45, 356–364.
 11. Chen, H., Zhang, M., Kong, F., Li, B., Cui, X., Huang, Y., Hort, N., Willumeit-Römer, R., Xie, W., & Wei, G. (2023). Effect of extrusion and rotary swaging on the microstructural evolution and properties of Mg-5Li-5.3Al-0.7Si alloy. *Materials Science and Engineering: A*, 885, 145627.
 12. Singh, N., Agrawal, M. K., Verma, S. K., & Tiwari, A. (2023). A review on impact route process on AA5083 of back pressure through equal channel angular pressing. *Materials Today: Proceedings*.
 13. Zhang, A. X., Li, F., Da Huo, P., Niu, W. T., & Gao, R. H. (2023). Response mechanism of matrix microstructure evolution and mechanical behavior to Mg/Al composite plate by hard-plate accumulative roll bonding. *Journal of Materials Research and Technology/Journal of Materials Research and Technology*, 23, 3312–3321.
 14. Tolouei, E., Toroghinejad, M. R., Mehr, V. Y., & Monajati, H. (2023). A combination of aluminium strip and brass mesh to process a refined structure composite via accumulative roll bonding: A characterization study. *Materials Characterization*, 205, 113360.

15. Parvin, H., & Kazeminezhad, M. (2023). Strength evolution during accumulative roll bonding of the metal matrix composite. *Journal of Materials Research and Technology/Journal of Materials Research and Technology*, 24, 1513–1523.
16. Dong, H., Chen, Y., Guo, Y., Shan, G., Yang, G., Huang, L., Liu, F., & Li, Q. (2023). A nanostructured Ag/Cu multilayered composite exhibiting high hardness and high electrical conductivity prepared by a novel multicomponent accumulative roll bonding. *Materials Characterization*, 196, 112613.
17. Wu, Q., Zhu, S., Wang, L., Liu, Q., Yue, G., Wang, J., & Guan, S. (2012). The microstructure and properties of cyclic extrusion compression treated Mg–Zn–Y–Nd alloy for vascular stent application. *Journal of the Mechanical Behavior of Biomedical Materials/Journal of Mechanical Behavior of Biomedical Materials*, 8, 1–7.
18. Chen, Y., Wang, Q., Roven, H., Karlsen, M., Yu, Y., Liu, M., & Hjelen, J. (2008). Microstructure evolution in magnesium alloy AZ31 during cyclic extrusion compression. *Journal of Alloys and Compounds*, 462(1–2), 192–200.
19. Lin, J., Wang, Q., Peng, L., & Roven, H. J. (2009). Microstructure and high tensile ductility of ZK60 magnesium alloy processed by cyclic extrusion and compression. *Journal of Alloys and Compounds*, 476(1–2), 441–445.
20. Zhang, L., Wang, Q., Liao, W., Guo, W., Li, W., Jiang, H., & Ding, W. (2017). Microstructure and mechanical properties of the carbon nanotubes reinforced AZ91D magnesium matrix composites processed by cyclic extrusion and compression. *Materials Science and Engineering. A, Structural Materials: Properties, Microstructures and Processing/Materials Science &*

Engineering. A, Structural Materials: Properties, Microstructure and Processing, 689, 427–434.

21. Hashemi, M., Alizadeh, R., & Langdon, T. G. (2023). Recent advances using equal-channel angular pressing to improve the properties of biodegradable Mg–Zn alloys. *Journal of Magnesium and Alloys*, 11(7), 2260–2284.
22. Yang, W., Quan, G., Ji, B., Wan, Y., Zhou, H., Zheng, J., & Yin, D. (2022). Effect of Y content and equal channel angular pressing on the microstructure, texture and mechanical property of extruded Mg-Y alloys. *Journal of Magnesium and Alloys*, 10(1), 195–208.
23. Lee, S., Tazoe, K., Mohamed, I. F., & Horita, Z. (2015). Strengthening of AA7075 alloy by processing with high-pressure sliding (HPS) and subsequent aging. *Materials Science and Engineering. A, Structural Materials: Properties, Microstructures and Processing/Materials Science & Engineering. A, Structural Materials: Properties, Microstructure and Processing*, 628, 56–61.
24. Xue, K., Tian, Z., Xie, R., & Li, P. (2023). Effect of high pressure torsion on interfaces and mechanical properties of SiC/Al composite. *Vacuum*, 218, 112647.
25. Chen, C., Hua, A., Yu, J., Chen, Y., Ji, W., & Qian, C. (2023). Mechanical alloying and phase transition of immiscible Al/Zn system during high-pressure torsion. *Transactions of Nonferrous Metals Society of China/Transactions of Nonferrous Metals Society of China*, 33(12), 3612–3624.
26. Sahu, S., Harris, J., Hamilton, A. R., & Gao, N. (2024). Interfacial characteristics of multi-material SS316L/IN718 fabricated by laser powder

- bed fusion and processed by high-pressure torsion. *Journal of Manufacturing Processes*, 110, 52–69.
27. Tian, T., Xu, H., Zhan, W., Zhang, Y., & Zhang, Q. (2023). Failure analysis of cold rotary swaging die. *Engineering Failure Analysis*, 153, 107580.
28. Chlupová, A., Šulák, I., Kunčická, L., Kocich, R., & Svoboda, J. (2021). Microstructural aspects of new grade ODS alloy consolidated by rotary swaging. *Materials Characterization*, 181, 111477.
29. Herrmann, M., Schenck, C., Leopold, H., & Kuhfuss, B. (2020). Material improvement of mild steel S355J2C by hot rotary swaging. *Procedia Manufacturing*, 47, 282–287.
30. Pachla, W., Kulczyk, M., Przybysz, S., Skiba, J., Wojciechowski, K., Przybysz, M., Topolski, K., Sobolewski, A., & Charkiewicz, M. (2015). Effect of severe plastic deformation realized by hydrostatic extrusion and rotary swaging on the properties of CP Ti grade 2. *Journal of Materials Processing Technology*, 221, 255–268.
31. Cheng, L., Zhang, X., Xu, J., Olugbade, T. O., Li, G., Dong, D., Lyu, F., Kong, H., Huo, M., & Lu, J. (2024). Nickel-based superalloy architectures with surface mechanical attrition treatment: Compressive properties and collapse behaviour. *Nano Materials Science*.
32. Cui, G., Bao, C., Zhang, M., & Zhang, X. (2022). Effects of thermal aging on mechanical properties and microstructures of an interstitial high entropy alloy with ultrasonic surface mechanical attrition treatment. *Materials Science and Engineering. A, Structural Materials: Properties, Microstructures and Processing/Materials Science & Engineering. A, Structural Materials: Properties, Microstructure and Processing*, 838, 142755.

33. Zhou, W., Apkarian, R., Wang, Z. L., & Joy, D. (2006). Fundamentals of Scanning Electron Microscopy (SEM). In *Springer eBooks* (pp. 1–40).
34. Tian, S., Zhao, Y., Dong, K., Liu, G., Yang, Q., & Li, L. (2021). Internal flow and cavitation analysis of Scroll oil pump by CFD Method. *Processes*, 9(10), 1705.
35. Becker, W. (1966). The turbomolecular pump, its design, operation and theory; calculation of the pumping speed for various gases and their dependence on the forepump. *Vacuum*, 16(11), 625–632.
36. Ratnayaka, D. D., Brandt, M. J., & Johnson, K. M. (2009). Valves and meters. In *Elsevier eBooks* (pp. 599–629).
37. Bonard, J., Dean, K. A., Coll, B. F., & Klinke, C. (2002). Field emission of individual carbon nanotubes in the scanning electron microscope. *Physical Review Letters*, 89(19).
38. Crewe, A. V., Wall, J., & Welter, L. M. (1968). A High-Resolution Scanning transmission electron microscope. *Journal of Applied Physics*, 39(13), 5861–5868.
39. Tensile testing. (2004). In *ASM International eBooks*.
40. Navaneetha, E., & Lakshmi, A. A. (2023). Cold extrusion on bulk materials: A review. *Materials Today: Proceedings*.
41. Michael Dunlap. , & Dr.J.E.Adaskaveg (1997). Introduction to the Scanning Electron Microscope Theory, Practice & Procedures.
42. Ken Arnold and Maurice Stewart (1998). Surface Production Operations. Gulf Professional Publishing.